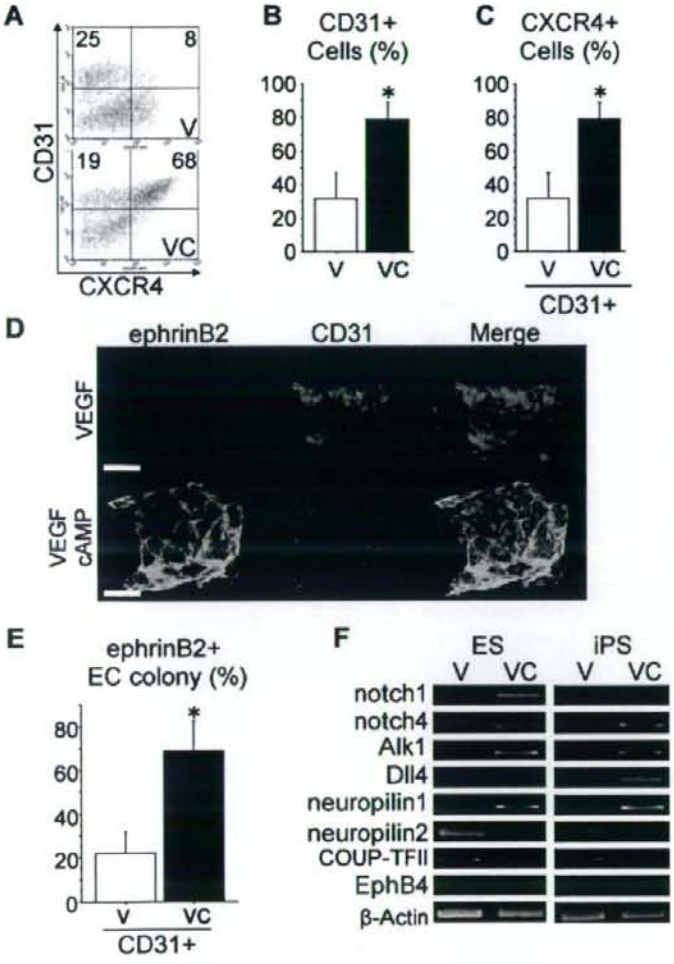

Figure 4. Arterial and venous EC induction from iPS cell–derived Flk1$^+$ cells. A, Representative results of FACS analysis for CD31 and CXCR4 (arterial EC marker) at Flk-d3. VEGF treatment alone (100 ng/mL) (V; top panel) and VEGF with 8bromo-cAMP (0.5 mmol/L) (VC; bottom panel) are shown. Percentages of venous ECs (CD31$^+$/CXCR4$^-$ population) and arterial ECs (CD31$^+$/CXCR4$^+$ population) are indicated. B, Percentages of CD31$^+$ cells (total ECs) in total Flk1$^+$ cell–derived cells (n=3; *P=0.02). C, Percentages of CD31$^+$/CXCR4$^+$ cells (arterial ECs) in total CD31$^+$ cells (n=3; *P=0.01). D, Double immunostaining for ephrinB2 (arterial ECs) (left panels, green) and CD31 (middle panels, red). Right panels show merged images with DAPI (blue). VEGF treatment alone (top) and VEGF with 8bromo-cAMP (bottom) are shown. E, Percentages of ephrinB2$^+$ arterial EC colonies in CD31$^+$ EC colonies (n=4; *P=0.009). F, Gene expressions of arterial and venous EC markers (reverse transcription polymerase chain reaction) in purified CD31$^+$/VE-cadherin$^+$ ECs. Scale bars=100 μm. ES cells (EB5; left) and iPS cells (20D17; right) are shown.

sisted mainly of CD31$^+$ ECs (Figure 3G). Attachment of SMA$^+$ mural cells to endothelial tubes was observed (Figure 3H; Figure III in the online-only Data Supplement), similar to our previous report with the use of ES cells.[4]

Arterial and Venous EC Induction From iPS Cells

We further examined arterial and venous EC differentiation. We recently reported that whereas VEGF treatment alone on Flk1$^+$ cells mainly induced venous ECs, activation of the cAMP pathway increased the total appearance of ECs and potently induced arterial ECs.[11] Figure 4A shows the results of the FACS analysis of Flk1$^+$ cell–derived cells at Flk-d3. VEGF treatment alone mainly induced CD31$^+$/CXCR4$^-$ venous ECs (top panel). In contrast, addition of 8bromo-cAMP, an analogue of cAMP, together with VEGF increased the total CD31$^+$ EC population as well as CD31$^+$/CXCR4$^+$ arterial ECs (bottom panel). The percentage of total ECs (CD31$^+$) in total Flk1$^+$ cell–derived cells (Figure 4B) and percentage of arterial ECs (CD31$^+$/CXCR4$^+$) in total ECs (CD31$^+$) (Figure 4C) were increased by ≈2.5-fold after 8bromo-cAMP treatment, respectively. The efficiency of total EC and arterial EC induction from iPS cell–derived Flk1$^+$ cells was comparable to that in ES cells.[11] Expression of another arterial EC marker, ephrinB2, was examined by immunostaining with the use of EphB4-Fc chimeric protein.[11] 8Bromo-cAMP treatment induced ephrinB2$^+$ arterial ECs (Figure 4D). The number of EC colonies including ephrinB2$^+$ arterial ECs increased ≈2.5-fold by 8bromo-cAMP treatment (Figure 4E). Gene expressions of other arterial and venous EC markers in FACS-purified ECs (CD31$^+$/VE-cadherin$^+$ population) further confirmed arterial and venous EC differentiation (Figure 4F), that is, an increase in arterial EC markers, such as notch1,4,[26] Alk1,[27] Dll4,[28] and neuropilin-1,[29] and a reciprocal decrease in venous EC markers, such as neuropilin-2,[30] COUP-TFII,[31] and EphB4,[32] were observed in VEGF and 8bromo-cAMP–induced ECs, paralleling ES and iPS cells. These results indicate that iPS cells possess the same properties as ES cells for arterial and venous EC differentiation.

iPS Cell Differentiation to Lymphatic ECs

We recently succeeded in inducing lymphatic ECs from mouse ES cells by culturing Flk1$^+$ cells on OP9 stroma cells

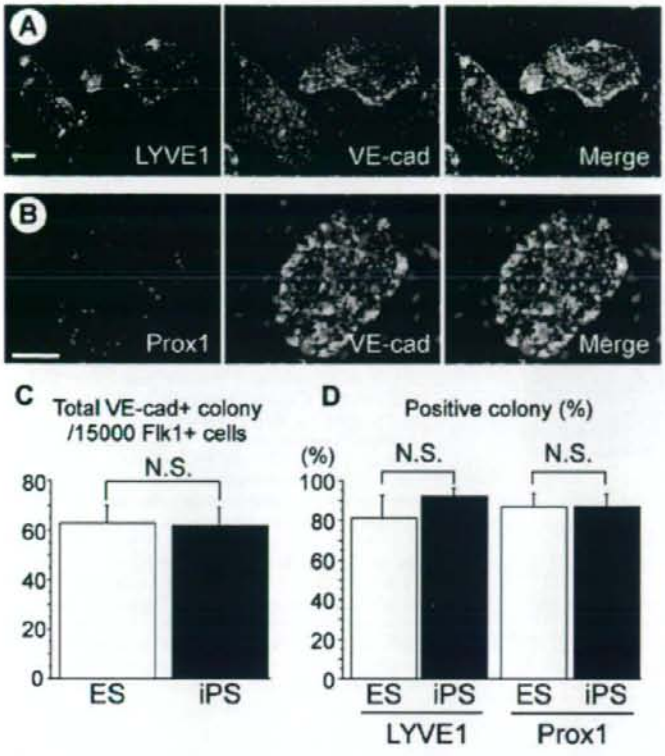

Figure 5. Differentiation of lymphatic ECs from iPS cells. A and B, Double immunostaining of LYVE1 (A) or prox1 (B) (lymphatic ECs; left panels, orange) and VE-cadherin (pan-ECs; middle panels, green) at Flk-d3 on OP9 cells. Right panels, Merged images with DAPI (blue). Bars=100 μm. C, Colony numbers of VE-cadherin (VE-cad)$^+$ ECs induced from 15 000 Flk1$^+$ cells (n=6). N.S. indicates not significant. P=0.86, ES cells (EB5) vs iPS cells (20D17). D, Percentages of EC colonies including lymphatic EC marker–positive cells in total EC colonies (n=3). P=0.89 (LYVE1), P=0.94 (Prox1), ES cells (EB5) vs iPS cells (20D17).

for 3 to 4 days[12] (Figure 1B). When iPS cell–derived Flk1$^+$ cells were cultured on OP9 cells, VE-cadherin$^+$ EC sheets appeared at Flk-d3. Most of the EC colonies that appeared were positive for lymphatic EC markers LYVE-1[33] and prox1[34] (Figure 5A and 5B). The induction efficiency of total EC colonies (VE-cadherin$^+$) (Figure 5C) and lymphatic EC$^+$ colonies (LYVE1$^+$ or prox1$^+$) (Figure 5D) on OP9 cells was comparable between ES and iPS cells, indicating that lymphatic ECs could also be similarly induced from iPS cells.

iPS Cell Differentiation to Cardiomyocytes

Finally, we performed induction of cardiomyocytes from iPS cells. To induce cardiomyocytes, we applied our 2-dimensional cardiomyocyte induction system of ES cells[5] to iPS cells. Similar to ES cells, when purified iPS cell–derived Flk1$^+$ cells were cocultured on OP9 cells, self-beating cardiomyocyte colonies appeared from Flk-d4-5 (Figure 1B) (Movie II in the online-only Data Supplement). Some beating colonies continued to beat for >2 months of culture. These beating colonies were positive for cTnT (Figure 6A). Although the numbers of beating colonies at Flk-d4–6 that appeared from 3 Nanog-iPS cell lines were slightly fewer than those from the EB5 ES cell line,[5] they were still more than those from another ES cell line, D3 cells (Figure 6B; Tables II and III in the online-only Data Supplement). The induction efficiency of cardiomyocytes from iPS cells was further quantitatively evaluated by FACS with the use of TMRM fluorescent dye.[17,18] Approximately half of MHC-GFP$^+$ cardiomyocytes induced from EMG7 ES cells could be detected as a TMRM-high population (Figure IA in the online-only Data Supplement). Being parallel to the beating colony number, the percentages of TMRM-high population induced from Flk1$^+$ cells with the use of EMG7 ES cells, 20D17 iPS cells, and D3 ES cells were 7.9%, 2.5%, and 0.9%, respectively (Figure IB and IC in the online-only Data Supplement). These results indicate that comparable levels of cardiomyocytes could be induced from iPS cells with ES cells. The difference of cardiogenic potentials is likely to be due to variation among cell clones and not due to features of iPS cells per se. Various cardiac marker genes, such as broad cardiomyocyte markers Nkx2.5 and α-MHC, atrial and ventricular myosin light chain 2, pacemaker marker, hyperpolarization-activated cyclic nucleotide-gated channel 4 (HCN4), and the conduction system marker connexin 40 appeared similarly in differentiation culture of ES and iPS cells on OP9 cells (Figure 6C). Various other features of cardiomyocytes were also observed in purified TMRM-high cells from iPS cells (Figure II in the online-only Data Supplement). Apparent sarcomere formation was detected by actinin staining (Figure 6D). A gap junction protein, connexin 43, was confirmed to be coexpressed with cTnT (Figure 6E). HCN4 and the T-type calcium channel Cav3.2, which were expressed in mouse sinoatrial node and important for automaticity of ES cell–derived cardiomyocytes,[35] also coexisted in cTnT$^+$ cardiomyocytes (Figure 6F and 6G). An atrial and ventricular ion channel, Kir2.1, was observed in cTnT$^+$ cells (Figure 6H). Some of the purified TMRM-high cardiomyocytes showed typical pacemaker-like potential and depolar-

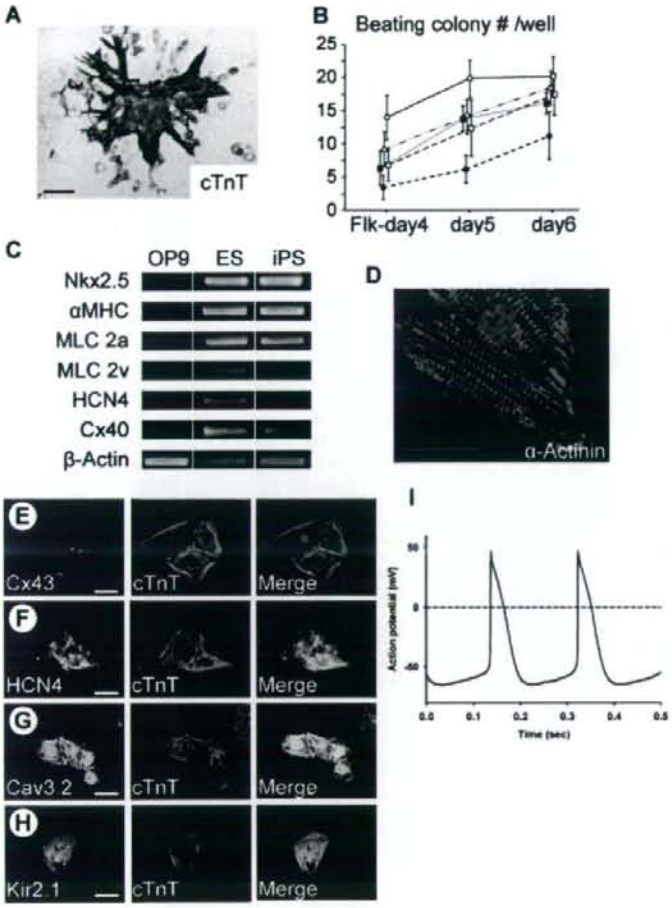

Figure 6. Cardiomyocyte differentiation from iPS cells. A, iPS cell–derived cardiomyocytes on OP9 cells at Flk-d6; cTnT staining (brown). B, Numbers of beating colonies at Flk-d4–6. EB5 ES cells (open circle), D3 ES cells (closed circle), 20D17 iPS cells (closed square), 38C2 iPS cells (open square), and 38D2 iPS cells (open triangle) (n=7) are shown. Averages and statistical analysis are shown in Tables II and III in the online-only Data Supplement. C, Gene expressions of various cardiomyocyte markers in cells at Flk-d6 on OP9 cells (reverse transcription polymerase chain reaction). OP9 cells (left), ES cells (EB5; middle), and iPS cells (20D17; right) are shown. D, Sarcomeric organization in TMRM-purified cardiomyocytes at Flk-d8. Immunostaining with anti-sarcomeric α-actinin antibody (red) and DAPI (blue). E to H, Double immunostaining of connexin43 (Cx43) (E), HCN4 (F), Cav3.2 (G), or Kir2.1 (H) (left, green) and cTnT (middle, orange) in TMRM-purified cardiomyocytes at Flk-d8. Right panels, Merged images with DAPI (blue). I, Representative action potential of iPS cell–derived self-beating cardiomyocytes. Bar=100 μm (A), 25 μm (D), 50 μm (E to H).

ized spontaneously (Figure 6I). Beating rate was 3.59±1.08 Hz, minimum potential was −66.89±6.07 mV, and maximum potential was 44.34±3.58 mV assessed by whole-cell patch clamp method (n=8). These results indicate that iPS cells also can differentiate into various cardiac cell types similar to ES cells.

Discussion

In this report, we showed that various cardiovascular cells could be directionally and systematically induced from mouse iPS cells. $CD45^+$ hematopoietic cells were also induced from iPS cell–derived $Flk1^+$ cells by coculturing with OP9 cells for 3days (Figure IV in the online-only Data Supplement). Thus, we succeeded in establishing a systematic culture system of iPS cells to reproduce differentiation and diversification processes of cardiovascular cells in vitro (Figure 7), which is useful in dissecting the process at the cellular level. The molecular mechanisms of iPS cell differentiation, including genetic and epigenetic aspects, can be examined with this system. This system would greatly contribute to the understanding of iPS cell biology and the development of new cardiovascular regenerative medicines.

During cardiovascular cell differentiation in this system, the properties of ES cells and iPS cells for time course, potential, and efficiency of differentiation were comparable. The physiological function of induced cardiomyocytes also showed no apparent difference between ES and iPS cells. These results suggest that iPS cells were completely reprogrammed and obtained pluripotent differentiation capacities as ES cells. In terms of the differentiation study, ES cells and iPS cells are principally identical, and methodologies obtained from ES cell studies can be applicable to iPS cells and vice versa.

iPS cells were originally induced by retrovirus-mediated transduction of 4 transcription factors, Oct3/4, Sox2, Klf4, and c-myc. It was reported that tumor formation was often observed in iPS cell–derived mice through the reexpression of the c-myc transgene.[16] When we examined mRNA expressions of the transgenes during long-term differentiation culture of $Flk1^+$ cells on OP9, the expression patterns were not constant. Occasionally, we observed upregulation of transgene mRNAs including c-myc after 1- or 2-month cultures (Figure V in the online-only Data Supplement). No apparent reappearance of undifferentiated or tumor cell–like structures were observed in the in vitro culture. Regulation of transgene

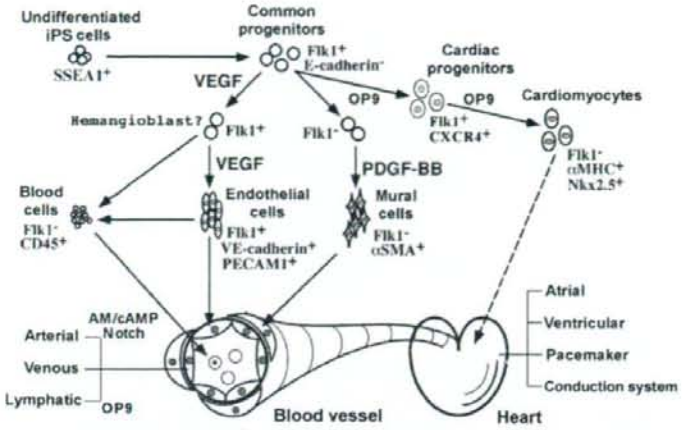

Figure 7. Systematic differentiation system of cardiovascular cells from iPS cells. Mouse iPS cell–derived Flk1$^+$ cells give rise to ECs in the presence of VEGF. VEGF alone induces ephrinB2$^-$ (EphB4$^+$) venous ECs. When cAMP signaling is activated together with VEGF, ephrinB2$^+$ arterial ECs are induced. For lymphatic EC differentiation, OP9 stroma cells are required. When Flk1$^+$ cells are cultured on OP9 stroma cells for 4 to 5 days, cardiomyocytes are induced as a mixture of various cardiac cell types: atrial, ventricular, pacemaker, and conduction system cells. CD45$^+$ blood cells are also induced from Flk1$^+$ cells cultured on OP9 cells. Various cardiovascular cells are therefore systematically induced from common progenitor Flk1$^+$ cells of mouse iPS cells. SSEA1 indicates stage-specific embryonic antigen.

expression should be different among iPS cell lines and modified by various factors, such as integration sites, copy numbers, epigenetic modifications of transgenes, and culture conditions. Although novel iPS cell induction methods devoid of the c-myc transgene have been reported recently,[36,37] retroviral transduction causes genomic insertion of transgenes, which may trigger tumor formation. The safety of iPS cells in regard to tumor formation should therefore be confirmed in each iPS cell line both in vitro and in vivo.

We successfully developed a cardiovascular differentiation system for mouse iPS cells and compared the differentiation properties of ES and iPS cells. Recently, we developed a similar vascular cell differentiation system using human ES cells[38] and applied that to vascular regeneration.[39] These differentiation systems for pluripotent stem cells would be applicable to human iPS cells and would greatly contribute to the generation of new-mode cardiovascular regenerative medicine with the use of iPS cells.

Acknowledgments

We thank Dr K. Takahashi for supporting and supervising iPS cell culture and Dr M. Takahashi for critical reading of the manuscript.

Sources of Funding

This study was supported by grants from the Ministry of Education, Science, Sports, and Culture of Japan; New Energy and Industrial Development Organization of Japan; Novartis Foundation for the Promotion of Science; Terumo Life Science Foundation; Yasuda Medical Foundation; and the Astellas Foundation for Research on Metabolic Disorders.

Disclosures

None.

References

1. Takahashi K, Yamanaka S. Induction of pluripotent stem cells from mouse embryonic and adult fibroblast cultures by defined factors. *Cell*. 2006;126:663–676.
2. Takahashi K, Tanabe K, Ohnuki M, Narita M, Ichisaka T, Tomoda K, Yamanaka S. Induction of pluripotent stem cells from adult human fibroblasts by defined factors. *Cell*. 2007;131:861–872.
3. Yu J, Vodyanik MA, Smuga-Otto K, Antosiewicz-Bourget J, Frane JL, Tian S, Nie J, Jonsdottir GA, Ruotti V, Stewart R, Slukvin II, Thomson JA. Induced pluripotent stem cell lines derived from human somatic cells. *Science*. 2007;318:1917–1920.
4. Yamashita J, Itoh H, Hirashima M, Ogawa M, Nishikawa S, Yurugi T, Naito M, Nakao K, Nishikawa S. Flk1-positive cells derived from embryonic stem cells serve as vascular progenitors. *Nature*. 2000;408:92–96.
5. Yamashita JK, Takano M, Hiraoka-Kanie M, Shimazu C, Peishi Y, Yanagi K, Nakano A, Inoue E, Kita F, Nishikawa SI. Prospective identification of cardiac progenitors by a novel single cell-based cardiomyocyte induction. *FASEB J*. 2005;19:1534–1536.
6. Yamashita J. Cardiovascular cell differentiation from ES cells. In: Mori H, Matsuda H, eds. *Cardiovascular Regeneration Therapies Using Tissue Engineering Approaches*. Tokyo, Japan: Springer-Verlag GmbH; 2004:67–80.
7. Yamaguchi T, Dumont D, Conlon R, Breitman M, Rossant J. Flk-1, an flt-related receptor tyrosine kinase is an early marker for endothelial cell precursors. *Development*. 1993;118:489–498.
8. Kataoka H, Takakura N, Nishikawa S, Tsuchida K, Kodama H, Kunisada T, Risau W, Kita T, Nishikawa SI. Expressions of PDGF receptor alpha, c-Kit and Flk1 genes clustering in mouse chromosome 5 define distinct subsets of nascent mesodermal cells. *Dev Growth Differ*. 1997;39:729–740.
9. Nishikawa SI, Nishikawa S, Hirashima M, Matsuyoshi N, Kodama H. Progressive lineage analysis by cell sorting and culture identifies FLK1$^+$VE-cadherin$^+$ cells at a diverging point of endothelial and hemopoietic lineages. *Development*. 1998;125:1747–1757.
10. Yamashita JK. Differentiation and diversification of vascular cells from embryonic stem cells. *Int J Hematol*. 2004;80:1–6.
11. Yurugi-Kobayashi T, Itoh H, Schroeder T, Nakano A, Narazaki G, Kita F, Yanagi K, Hiraoka-Kanie M, Inoue E, Ara T, Nagasawa T, Just U, Nakao K, Nishikawa SI, Yamashita JK. Adrenomedullin/cyclic AMP pathway induces notch activation and differentiation of arterial endothelial cells from vascular progenitors. *Arterioscler Thromb Vasc Biol*. 2006;26:1977–1984.
12. Kono T, Kubo H, Shimazu C, Ueda Y, Takahashi M, Yanagi K, Fujita N, Tsuruo T, Wada H, Yamashita JK. Differentiation of lymphatic endothelial cells from embryonic stem cells on OP9 stromal cells. *Arterioscler Thromb Vasc Biol*. 2006;26:2070–2076.
13. Yamashita JK. Differentiation of arterial, venous, and lymphatic endothelial cells from vascular progenitors. *Trends Cardiovasc Med*. 2007;17:59–63.
14. Matsuyoshi N, Toda K, Horiguchi Y, Tanaka T, Nakagawa S, Takeichi M, Imamura S. In vivo evidence of the critical role of cadherin-5 in murine vascular integrity. *Proc Assoc Am Physicians*. 1997;109:362–371.
15. Kodama H, Nose M, Niida S, Nishikawa S, Nishikawa S. Involvement of the c-kit receptor in the adhesion of hematopoietic stem cells to stromal cells. *Exp Hematol*. 1994;22:979–984.
16. Okita K, Ichisaka T, Yamanaka S. Generation of germline-competent induced pluripotent stem cells. *Nature*. 2007;448:313–317.
17. Hattori F, Chen H, Li W, Yuasa S, Onitsuka T, Shimoji K, Sasaki E, Ogawa S, Oikawa T, Fukuda K. Mitochondrial membrane potential measurement dye is applicable for the purification of mouse and marmoset embryonic stem cell-derived cardiomyocytes. *Circ J*. 2007;71(suppl I):465.

18. Scaduto RC, Grotyohann LW. Measurement of mitochondrial membrane potential using fluorescent rhodamine derivatives. *Biophys J*. 1999;76: 469–477.
19. Mitsui K, Tokuzawa Y, Itoh H, Segawa K, Murakami M, Takahashi K, Maruyama M, Maeda M, Yamanaka S. The homeoprotein Nanog is required for maintenance of pluripotency in mouse epiblast and ES cells. *Cell*. 2003;113:631–642.
20. Niwa H, Miyazaki J, Smith AG. Quantitative expression of Oct-3/4 defines differentiation, dedifferentiation or self-renewal of ES cells. *Nat Genet*. 2000;24:372–376.
21. Nichols J, Zevnik B, Anastassiadis K, Niwa H, Klewe-Nebenius D, Chambers I, Scholer H, Smith A. Formation of pluripotent stem cells in the mammalian embryo depends on the POU transcription factor Oct4. *Cell*. 1998;95:379–391.
22. Kubo A, Shinozaki K, Shannon JM, Kouskoff V, Kennedy M, Woo S, Fehling HJ, Keller G. Development of definitive endoderm from embryonic stem cells in culture. *Development*. 2004;131:1651–1662.
23. Laugwitz KL, Moretti A, Caron L, Nakano A, Chien KR. Islet1 cardiovascular progenitors: a single source for heart lineages? *Development*. 2008;135:193–205.
24. Lints T, Parsons L, Hartley L, Lyons I, Harvey R. Nkx-2.5: a novel murine homeobox gene expressed in early heart progenitor cells and their myogenic descendants. *Development*. 1993;119:419–431.
25. Komuro I, Izumo S. Csx: a murine homeobox-containing gene specifically expressed in the developing heart. *Proc Natl Acad Sci U S A*. 1993;90:8145–8149.
26. Villa N, Walker L, Lindsell C, Gasson J, Iruela-Arispe M, Weinmaster G. Vascular expression of Notch pathway receptors and ligands is restricted to arterial vessels. *Mech Dev*. 2001;108:161–164.
27. Seki T, Yun J, Oh S. Arterial endothelium-specific activin receptor-like kinase 1 expression suggests its role in arterialization and vascular remodeling. *Circ Res*. 2003;93:682–689.
28. Duarte A, Hirashima M, Benedito R, Trindade A, Diniz P, Bekman E, Costa L, Henrique D, Rossant J. Dosage-sensitive requirement for mouse Dll4 in artery development. *Genes Dev*. 2004;18:2474–2478.
29. Mukouyama Y, Shin D, Britsch S, Taniguchi M, Anderson D. Sensory nerves determine the pattern of arterial differentiation and blood vessel branching in the skin. *Cell*. 2002;109:693–705.
30. Yuan L, Moyon D, Pardanaud L, Bréant C, Karkkainen MJ, Alitalo K, Eichmann A. Abnormal lymphatic vessel development in neuropilin 2 mutant mice. *Development*. 2002;129:4797–4806.
31. You L, Lin F, Lee C, DeMayo F, Tsai M, Tsai S. Suppression of Notch signalling by the COUP-TFII transcription factor regulates vein identity. *Nature*. 2005;435:98–104.
32. Wang H, Chen Z, Anderson D. Molecular distinction and angiogenic interaction between embryonic arteries and veins revealed by ephrin-B2 and its receptor Eph-B4. *Cell*. 1998;93:741–753.
33. Jain R, Padera T. Development: lymphatics make the break. *Science*. 2003;299:209–210.
34. Wigle J, Harvey N, Detmar M, Lagutina I, Grosveld G, Gunn M, Jackson D, Oliver G. An essential role for Prox1 in the induction of the lymphatic endothelial cell phenotype. *EMBO J*. 2002;21:1505–1513.
35. Yanagi K, Takano M, Narazaki G, Uosaki H, Hoshino T, Ishii T, Misaki T, Yamashita JK. Hyperpolarization-activated cyclic nucleotide-gated channels and T-type calcium channels confer automaticity of embryonic stem cell-derived cardiomyocytes. *Stem Cells*. 2007;25:2712–2719.
36. Nakagawa M, Koyanagi M, Tanabe K, Takahashi K, Ichisaka T, Aoi T, Okita K, Mochiduki Y, Takizawa N, Yamanaka S. Generation of induced pluripotent stem cells without Myc from mouse and human fibroblasts. *Nat Biotechnol*. 2008;26:101–106.
37. Aoi T, Yae K, Nakagawa M, Ichisaka T, Okita K, Takahashi K, Chiba T, Yamanaka S. Generation of pluripotent stem cells from adult mouse liver and stomach cells. *Science*. In press.
38. Sone M, Itoh H, Yamahara K, Yamashita JK, Yurugi-Kobayashi T, Nonoguchi A, Suzuki Y, Chao TH, Sawada N, Fukunaga Y, Miyashita K, Park K, Oyamada N, Sawada N, Taura D, Tamura N, Kondo Y, Nito S, Suemori H, Nakatsuji N, Nishikawa S, Nakao K. Pathway for differentiation of human embryonic stem cells to vascular cell components and their potential for vascular regeneration. *Arterioscler Thromb Vasc Biol*. 2007;27:2127–2134.
39. Yamahara K, Sone M, Itoh H, Yamashita JK, Yurugi-Kobayashi T, Homma K, Chao TH, Miyashita K, Park K, Oyamada N, Sawada N, Taura D, Tamura N, Nakao K. Augmentation of neovascularization in hindlimb ischemia by combined transplantation of human embryonic stem cells-derived endothelial and mural cells. *PLoS One*. 2008;3:e1666.

CLINICAL PERSPECTIVE

The recent invention of skin fibroblast-derived pluripotent cells, induced pluripotent stem (iPS) cells, opened a new gate for regenerative medicine. Establishment of iPS cells from adult human tissue is further facilitating development of cell transplantation–based regenerative strategies by avoiding the legal and ethical controversy over human embryonic stem cells. This study discusses a directed and systematic differentiation method of using mouse iPS cells for various cardiovascular cells, which would provide a scientific and technological basis for human iPS cell differentiation. As well as the direct application to cell-based regenerative medicine, this study also examines and elucidates the cellular and molecular mechanisms of cardiovascular cell differentiation, thereby contributing to identify novel targets for gene therapy and drug discovery. Furthermore, this system could be directly involved in screening of small molecules to find cardiovascular regenerating substances. This study therefore may greatly contribute to the clinical application of iPS cells and develop novel regenerative medicine for cardiovascular diseases.

Available online at www.sciencedirect.com
ScienceDirect
Bioorganic & Medicinal Chemistry Letters 18 (2008) 2982–2984
Bioorganic & Medicinal Chemistry Letters

Evaluation of antiangiogenic activity of azumamides by the in vitro vascular organization model using mouse induced pluripotent stem (iPS) cells

Yoichi Nakao,[a,*] Genta Narazaki,[b] Takuhiro Hoshino,[b] Satoko Maeda,[c] Minoru Yoshida,[c] Hiroshi Maejima[a] and Jun K. Yamashita[b,*]

[a]*Department of Chemistry and Biochemistry, Waseda University, 3-4-1 Okubo, Shinjuku-ku, Tokyo 169-8555, Japan*
[b]*Institute for Frontier Medical Sciences, Kyoto University, Kyoto 606-8507, Japan*
[c]*Chemical Genetics Laboratory, RIKEN, Saitama 351-0198, Japan*

Received 12 February 2008; revised 3 March 2008; accepted 18 March 2008
Available online 21 March 2008

Abstract—Evaluation of antiangiogenic activity of marine sponge derived azumamides by the in vitro vascular organization model using mouse induced pluripotent stem (iPS) cells was carried out. Azumamide E (**5**) strongly inhibited in vitro angiogenesis from iPS cells at 1.9 μM while azumamide A (**1**) showed only weak inhibition at 19 μM. These results were well correlated with HDAC inhibitory activity of these compounds, revealing the prospect of azumamides as the probe molecules useful for stem cell chemical biology.

The establishment of mouse induced pluripotent stem (iPS) cells[1] followed by the success in reprogramming of differentiated human somatic cells into a pluripotent state[2,3] gave a significant impact on the life sciences not only because of the possibility of regeneration therapy without rejection associated with traditional transplantation but also because of the prospect for application to the assay systems evaluating efficacy and toxicity of drugs against the individual SNP. Therefore, it seems to be an urgent issue to verify the biological activity of the probe molecules found by the assay using ES cells in the iPS systems for further development of stem cell biology by means of chemical biological strategy.

Azumamides A–E (**1**–**5**) are the histone deacetylase (HDAC) inhibitors isolated from the marine sponge *Mycale izuensis*.[4,5] Consistent with the former report that HDACs can be the promising target of antiangiogenic therapy,[6,7] azumamide A (**1**) was also found to inhibit vascularization in the in vitro vascular organization model using mouse ES cells at 19 μM.[8]

Since the following studies[9,10] revealed that the HDAC inhibitory activity of synthetic **1** was not as potent as that of originally reported while synthetic **5** retained the equivalent potency, we re-evaluated inhibitory activities of **1**–**5** against HDAC1, HDAC4, and HDAC6, as well as p21 promotion activities. Then, the antiangiogenic activities of azumamides A (**1**) and E (**5**) by the in vitro vascular organization model using mouse induced pluripotent stem (iPS) cells were tested. As a result, we found a dose-dependent antiangiogenic activity in the iPS cell system of **5**, while **1** showed only a moderate effect.

These results were well correlated with their HDAC inhibitory activities, and therefore, azumamide E (**5**) is presumed to be the promising probe molecule for the chemical biology of angiogenesis and stem cell differentiation.

Azumamides A–E were assayed for HDAC inhibitory activity using HDAC1, HDAC4, and HDAC6 enzymes prepared from 293T cells.[11] Azumamides A (**1**) and D (**4**) showed only a very weak inhibitory activity against

Keywords: iPS cells; Histone deacetylase; Angiogenesis; Chemical biology.
* Corresponding authors. Tel./fax: +81 3 5286 2568 (Y.N.); tel.: +81 75 751 3853; fax: +81 75 751 4824 (J.K.Y.); e-mail addresses: ayocha@waseda.jp; juny@frontier.kyoto-u.ac.jp

0960-894X/$ - see front matter © 2008 Published by Elsevier Ltd.
doi:10.1016/j.bmcl.2008.03.053

these subtypes at 50 μM, while B (**2**), C (**3**), and E (**5**) showed inhibitory activities against HDAC1 and HDAC4 with IC_{50} values ranging from 1.17 to 3.66 μM. None of **1**–**5** showed remarkable activity against HDAC6. Promotion of p21 expression was also evaluated[12] and only azumamide E (**5**) showed a moderate activity with EC_{1000} value of 17.0 μM (Table 1).

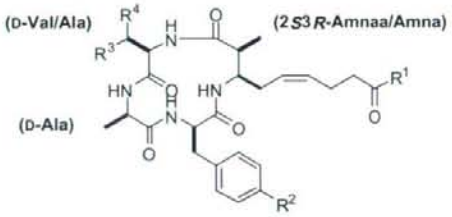

		R^1	R^2	R^3 = R^4
azumamide	A (1)	NH_2	H	Me
	B(2)	NH_2	OH	Me
	C(3)	OH	OH	Me
	D(4)	NH_2	H	H
	E(5)	OH	H	Me

These results suggested that azumamide E (**5**) is the most active among **1**–**5**, therefore, **1** and **5** were tested for their antiangiogenic activity in the in vitro vascular organization model using mouse iPS cells.[13]

Evaluation of antiangiogenic activity was carried out basically following the procedure using mouse ES cells,[4,8] except that mouse iPS cells derived from mouse skin fibroblasts were used instead of mouse ES cells.

In this model, azumamide A (**1**) did not show or showed only a weak inhibition even at 19 μM (Fig. 1c and g), which is inconsistent to the former result but consistent with the HDAC inhibitory activity (IC_{50} > 50 μM) obtained in this assay.

On the other hand, azumamide E (**5**) showed dose-dependent inhibition of angiogenesis in this model at as low as 0.19 μM (Fig. 2). The observed antiangiogenic activity of **5** was again well consistent with the inhibitory activity against HDAC1 and HDAC4.

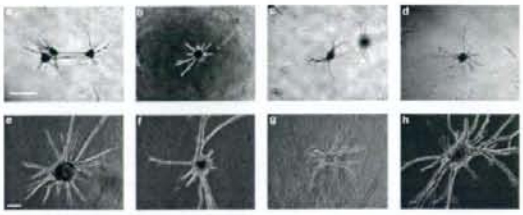

Figure 1. Effects of azumamide A (**1**) on in vitro vascular organization of mouse iPS cells. (a–d) ×4, bar = 500 μm. (e–h) ×10, bar = 100 μm. (a and e) 0.19 μM of **1**. (b and f) 1.9 μM of **1**. (c and g) 19 μM of **1**. (d and h) 0 μM of **1**.

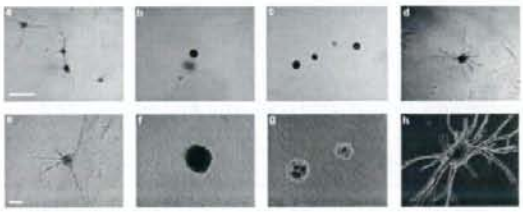

Figure 2. Effects of azumamide E (**5**) on in vitro vascular organization of mouse iPS cells. (a–d) ×4, bar = 500 μm. (e–h) ×10, bar = 100 μm. (a and e) 0.19 μM of **5**. (b and f) 1.9 μM of **5**. (c and g) 19 μM of **5**. (d and h) 0 μM of **5**.

In the present study, we have tested inhibitory activity of azumamides A–E (**1**–**5**) against HDAC1, HDAC4, and HDAC6, as well as p21 promotion activity. In the HDAC inhibitory assay system used in this study, azumamides showed weaker activities than those obtained in the previous report.[4] Inhibitory activities obtained for the synthetic azumamides by Ganesan[10] also showed a weaker activity of **1**. From the results of De Riccardis[9] and Ganesan,[10] it seems that assay conditions may largely affect the HDAC inhibitory activities. However, the results of HDAC inhibition assay for azumamides A and E in the present study were well correlated with the antiangiogenic activity in the iPS cells system.

It will be a valid strategy for the stem cell chemical biology, to compare gene expression or epigenetic states during the cell differentiation processes under the different culture conditions prepared by the administration of positive or negative probe molecules, respectively. Azumamides A (**1**) and E (**5**) can be such a probe molecule

Table 1. Biological activity of azumamides A–E (**1**–**5**)

Compound	HDAC1[a]	HDAC4[a]	HDAC6[a]	p21 promotion[b]
1	>50 μM	>50 μM	>50 μM	>25 μM
2	1.83 μM ± 0.11	3.66 μM ± 1.34	>50 μM	>25 μM
3	1.17 μM ± 0.16	3.16 μM ± 0.21	>50 μM	>25 μM
4	>50 μM	>50 μM	>50 μM	>25 μM
5	1.22 μM ± 0.13	2.28 μM ± 0.16	>50 μM	17.0 μM ± 3.91
TSA[c]	0.0366 μM	0.0629 μM	0.0833 μM	0.0115 μM

[a] IC_{50} values (±standard deviation).
[b] EC_{1000} values.
[c] Trichostatin A.

set ideal for the chemical biological study of stem cell differentiation and angiogenesis using iPS cells.

Acknowledgments

This work was partly supported by the Waseda University Grant for Special Research Projects, the Nissui Research foundation, and a Grant-in-Aid for Scientific Research from the Ministry of Education, Culture, Sports, Science, and Technology of Japan.

Supplementary data

Supplementary data associated with this article can be found, in the online version, at doi:10.1016/j.bmcl.2008.03.053.

References and notes

1. Takahashi, K.; Yamanaka, S. *Cell* **2006**, *126*, 663.
2. Takahashi, K.; Tanabe, K.; Ohnuki, M.; Narita, M.; Ichisaka, T.; Tomoda, K.; Yamanaka, S. *Cell* **2008**, *131*, 1.
3. Yu, J.; Vodyanik, M. A.; Smuga-Otto, K.; Antosiewicz-Bourget, J.; Frane, J. L.; Tian, S.; Nie, J.; Jonsdottir, G. A.; Routti, V.; Stewart, R.; Slukvin, I. I.; Thomson, J. A. *Science* **2007**, *318*, 1917.
4. Nakao, Y.; Yoshida, S.; Matsunaga, S.; Shindoh, N.; Terada, Y.; Nagai, K.; Yamashita, J. K.; Ganesan, A.; van Soest, R. W. M.; Fusetani, N. *Angew. Chem., Int. Ed.* **2006**, *45*, 7553.
5. Izzo, I.; Maulucci, N.; Bifulco, G.; De Riccardis, F. *Angew. Chem., Int. Ed.* **2006**, *45*, 7557.
6. Qian, D. Z.; Kato, Y.; Shabbeer, S.; Wei, Y.; Verheul, H. M. W.; Salumbides, B.; Sanni, T.; Atadja, P.; Pili1, R. *Clin. Cancer Res.* **2006**, *12*, 634.
7. Chang, S.; Young, B. D.; Li, S.; Qi, X.; Richardson, J. A.; Olson1, E. N. *Cell* **2006**, *126*, 321.
8. Yamashita, J.; Itoh, H.; Hirashima, M.; Ogawa, M.; Nishikawa, S.; Yurugi, T.; Naito, M.; Nakao, K.; Nishikawa, S.-I. *Nature* **2000**, *408*, 92.
9. Maulucci, N.; Chini, M. G.; Di Micco, S.; Izzo, I.; Cafaro, E.; Russo, A.; Gallinari, P.; Paolini, C.; Nardi, M. C.; Casapullo, A.; Riccio, R.; Bifulco, G.; De Riccardis, F. *J. Am. Chem. Soc.* **2007**, *129*, 3007.
10. Wen, S.; Carey, K. L.; Nakao, Y.; Fusetani, N.; Packham, G.; Ganesan, A. *Org. Lett.* **2007**, *9*, 1105.
11. Shivashimpi, G. M.; Amagai, S.; Kato, T.; Nishino, N.; Maeda, S.; Nishino, T. G.; Yoshida, M. *Bioorg. Med. Chem.* **2007**, *15*, 7830.
12. Furumai, R.; Matsuyama, A.; Kobashi, N.; Lee, K.-H.; Nishiyama, M.; Nakajima, H.; Tanaka, A.; Komatsu, Y.; Nishino, N.; Yoshida, M.; Horinouchi, S. *Cancer Res.* **2002**, *62*, 4916.
13. Narazaki, G.; Teranishi, M.; Okita, K.; Yamanaka, S.; Yamashita, J. K. Presented at the 7th Congress of Japan Society for Regenerative Medicine, Nagoya, Japan, March 2008, paper o-21-1.

Augmentation of Neovascularizaiton in Hindlimb Ischemia by Combined Transplantation of Human Embryonic Stem Cells-Derived Endothelial and Mural Cells

Kenichi Yamahara[1☯], Masakatsu Sone[1☯], Hiroshi Itoh[1,2*], Jun K. Yamashita[3], Takami Yurugi-Kobayashi[3], Koichiro Homma[2], Ting-Hsing Chao[4], Kazutoshi Miyashita[1,2], Kwijun Park[1], Naofumi Oyamada[1], Naoya Sawada[1], Daisuke Taura[1], Yasutomo Fukunaga[1], Naohisa Tamura[1], Kazuwa Nakao[1]

1 Department of Medicine and Clinical Science, Kyoto University Graduate School of Medicine, Kyoto, Japan, **2** Department of Internal Medicine, Keio University School of Medicine, Tokyo, Japan, **3** Laboratory of Stem Cell Differentiation, Stem Cell Research Center, Institute for Frontier Medical Science, Kyoto University, Kyoto, Japan, **4** Division of Cardiology, Department of Internal Medicine, National Cheng Kung University Medical Center, Tainan, Taiwan

Abstract

Background: We demonstrated that mouse embryonic stem (ES) cells-derived vascular endothelial growth factor receptor-2 (VEGF-R2) positive cells could differentiate into both endothelial cells (EC) and mural cells (MC), and termed them as vascular progenitor cells (VPC). Recently, we have established a method to expand monkey and human ES cells-derived VPC with the proper differentiation stage in a large quantity. Here we investigated the therapeutic potential of human VPC-derived EC and MC for vascular regeneration.

Methods and Results: After the expansion of human VPC-derived vascular cells, we transplanted these cells to nude mice with hindlimb ischemia. The blood flow recovery and capillary density in ischemic hindlimbs were significantly improved in human VPC-derived EC-transplanted mice, compared to human peripheral and umbilical cord blood-derived endothelial progenitor cells (pEPC and uEPC) transplanted mice. The combined transplantation of human VPC-derived EC and MC synergistically improved blood flow of ischemic hindlimbs remarkably, compared to the single cell transplantations. Transplanted VPC-derived vascular cells were effectively incorporated into host circulating vessels as EC and MC to maintain long-term vascular integrity.

Conclusions: Our findings suggest that the combined transplantation of human ES cells-derived EC and MC can be used as a new promising strategy for therapeutic vascular regeneration in patients with tissue ischemia.

Citation: Yamahara K, Sone M, Itoh H, Yamashita JK, Yurugi-Kobayashi T, et al (2008) Augmentation of Neovascularizaiton in Hindlimb Ischemia by Combined Transplantation of Human Embryonic Stem Cells-Derived Endothelial and Mural Cells. PLoS ONE 3(2): e1666. doi:10.1371/journal.pone.0001666

Editor: Tailoi Chan-Ling, University of Sydney, Australia

Received November 5, 2007; **Accepted** January 24, 2008; **Published** February 27, 2008

Funding: This work is supported by a grant-in-aid for scientific research (the Japanese Ministry of Education, Culture, Sports, Science and Technology), a research grant from them 21st COE Program for Integration of Transplantation Therapy and Regenerative Medicine (Japan Society for the Promotion of Science), a research grant from the Project for Development of Regenerative Medicine (the Japanese Ministry of Education, Culture, Sports, Science and Technology), and a research grant from the Japan Foundation for Aging and Health (the Japanese Ministry of Health, Labor and Welfare).

Competing Interests: The authors have declared that no competing interests exist.

*E-mail: hrith@sc.itc.keio.ac.jp

☯These authors contributed equally to this work.

Introduction

Embryonic stem (ES) cells, with their extensive regeneration potential and functional multilineage differentiation capacity, are now highlighted as promising cell sources for regenerative medicine. Previously we reported that mouse ES cells-derived vascular endothelial growth factor receptor-2 (VEGFR2) positive cells could differentiate into both endothelial cells (EC) and mural cells (MC) (pericytes and vascular smooth muscle cells) and reproduce the vascular organization process, which we termed "vascular progenitor cells (VPC)" [1]. Transplanted VPC into tumor-bearing nude mice were incorporated into blood vessels and significantly increased blood flow, which suggests that VPC might be useful for augmenting vessel growth in ischemic tissue [2].

We have demonstrated that human as well as monkey ES cells possessed different differentiation kinetics of VPC derived from mouse ES cells [3,4]. In contrast to mouse ES cells, undifferentiated human ES cells already expressed VEGFR2. After the induction of differentiation on OP9 feeder cells, VEGFR2 positive and tumor rejection antigen-1 (TRA1: a marker indicative of undifferentiated cell phenotype) negative cells appeared at day 8. We confirmed that VEGFR2 positive cells at this stage effectively differentiated into both VE-cadherin positive EC and α-smooth muscle actin (αSMA) positive MC to suffice as human VPC.

Human VPC-derived VEGFR2$^+$ VE-cadherin$^+$ cells, which were considered as EC at an early differentiation stage, formed a network structure on Matrigel-coated dishes.

Based upon these works, in the present study we transplanted human VPC-derived vascular cells; that is, EC and MC in a murine hindlimb ischemia model. By transplantation of these EC and MC differentiated from human VPC, we investigated whether and how they could be incorporated as EC and MC into the sites of neovascularization, compared to human peripheral blood and umbilical cord blood-derived endothelial progenitor cell (EPC) transplantation [5–7]. Furthermore, we specifically asked whether the combined transplantation of human VPC-derived EC and MC could induce stable vascular regeneration to achieve long-term vascular integrity.

Results

Characterization of Transplanted Human VPC-derived Vascular Cells

Flow cytometric analysis disclosed that 20–40% of expanded human VPC-derived EC retained the expression of the endothelial cell-related markers, including VE-cadherin, VEGFR2, CD34, CD31 and CD105, and all of the cells were negative for a panleukocyte marker CD45, monocyte/macrophage marker (CD11b), and stem/progenitor makers (AC133 and c-kit) (Figure 1a). By the double immunostaining of CD31 and αSMA, the cells negative for CD31 were exclusively positive for αSMA (Figure 1b), but weak or negative for staining with other MC markers, including calponin, smooth muscle myosin heavy chain 1 (SM1) and 2 (SM2) (data not shown).

Immunocytochemistry of expanded human VPC-derived MC revealed that all these cells were positive for αSMA, calponin, SM1 and SM2 (Figure 1c). Analysis by reverse transcription-polymerase chain reaction (RT-PCR) also confirmed that mRNA expressions of these MC markers were upregulated in human VPC-derived MC and negative in sorted VE-cadherin$^+$ fraction of expanded human VPC-derived EC (Figure 1d). Although cultured human aortic smooth muscle cells (hAoSMC) expressed a high level of h-caldesmon, its expression in human VPC-derived MC was not detected. Furthermore, mRNA for skeletal (myogenin and MyoD) or cardiac (cardiac troponin T (cTnT) and I (cTnI)) specific marker was not detected in human VPC-derived MC (Figure 1e).

Characterization of Transplanted Human EPC

Flow cytometric analysis of pEPC demonstrated that these cells mainly exhibited two light-scattering properties: one was consistent with a relatively large cell size (gate P1) and the other was found in a smaller gate P2 (Figure 2a). The P1-gated cells were positive for DiI-acLDL uptake and ulex-lectin binding (Figure 2b), and exhibited the reported EPC phenotype [6,8]. However, the smaller P2-gated cells were low positive for DiI-acLDL/ulex-lectin (Figure 2c). Therefore, we performed subsequent fluorescence activated cell sorter (FACS) analysis of pEPC on the P1-gated cells.

As shown in Figure 2d, nearly all pEPC expressed the hematopoietic markers CD45 (99.9%) and CD54 (99.9%) and the monocyte/macrophage markers CD14 (99.0%), CD11b (98.7%), and CD11c (98.9%). The monocyte/macrophage or endothelial markers CD31 (58.3%) and CD105 (70.1%) were also expressed. A much lower percentage of these cells expressed the endothelial cell-related markers VE-cadherin (1.6%), VEGFR2 (5.4%), and von Willebrand Factor (vWF) (0.3%), or the stem/progenitor cell markers AC133 (1.0%), c-kit (0.4%), and CD34 (0.2%).

Flow cytometric analysis of magnetic cell separation system (MACS)-sorted uEPC showed more than 80% of these cells were positive for CD34 (data not shown). Similar to pEPC, almost all CD34$^+$ fraction of uEPC expressed the hematopoietic markers CD45 (99.0%) and CD54 (84.9%) (Figure 2e). However, the expression of monocyte/macrophage markers was limited in uEPC (CD14 5.7%, CD11b 99.7%, CD11c 21.3%), and significant number of these cells was positive for the endothelial cell-related markers, including VE-cadherin (11.2%), VEGFR2 (8.1%), and vWF (7.9%). In addition, these CD34$^+$ uEPC expressed the stem/progenitor markers AC133 (80.6%) and c-kit (95.3%).

Long-term Improvement of Blood Flow of Ischemic Hindlimb by Human VPC-derived Vascular Cell Transplantation

To examine the comparative effectiveness of transplanted human VPC-derived vascular cells for vascular regeneration, we set up six groups as follows (Figure 3);

1) EC+MC group (n = 9): the mixture of 0.5×10^6 human VPC-derived EC and 0.5×10^6 MC, with the total cell number of 1×10^6,
2) EC group (n = 20): 0.5×10^6 human VPC-derived EC,
3) MC group (n = 18): 0.5×10^6 human VPC-derived MC,
4) uEPC group (n = 10): 1×10^6 umbilical cord-derived CD34$^+$ cells,
5) pEPC group (n = 16): 1×10^6 peripheral mononuclear cells (MNC)-derived EPC,
6) Control group (n = 17): only 100 μl PBS.

To analyze subcutaneous hindlimb perfusion, laser Doppler perfusion image (LDPI) analysis was performed (Figure 4a). Throughout the 42 day follow-up period, significantly accelerated limb perfusion improvement was observed in the VPC-derived EC+MC-transplanted group, compared to the EPC and control groups (Figure 4b, $P<0.001$ vs. control, pEPC, uEPC, and MC groups, $P = 0.002$ vs. EC group, repeated measures ANOVA followed by Bonferoni's multiple comparison test).

At day 14, blood flow of the mice transplanted with EPC (the ratio of ischemic/non-ischemic blood flow: 0.907 ± 0.058 in pEPC and 0.942 ± 0.075 in uEPC) ($P = 0.035$ and 0.028, compared to the control group), as well as MC (0.957 ± 0.056) ($P = 0.006$) and EC (0.901 ± 0.063) ($P = 0.032$) showed significant increase, compared to the control group (0.730 ± 0.042) (Figure 4b). In the EC+MC group, the ratio of ischemic/non-ischemic blood flow markedly elevated to 1.187 ± 0.083 ($P<0.0001$), compared to other groups.

Blood flow in the pEPC group, however, did not increase thereafter and no significant difference in the blood flow between the pEPC and control group was seen at days 28 and 42 (Figure 4b). In the uEPC group, significant blood flow recovery was seen at day 42 (0.990 ± 0.054) ($P = 0.009$), compared to the control group (0.749 ± 0.039). The blood flow in the VPC-derived vascular cells-transplanted groups progressively increased. At day 42, the calculated perfusion ratio of ischemic to non-ischemic hindlimb significantly elevated to 0.943 ± 0.057 for the MC ($P = 0.013$), 1.038 ± 0.059 for the EC ($P = 0.0002$), and 1.231 ± 0.067 for the EC+MC group ($P<0.0001$) compared to the control group (0.749 ± 0.039). Between the cell mixture transplantation (EC+MC) group and the single cell transplantation (EC or MC) groups, the blood flow of ischemic hindlimbs was significantly different at day 42 ($P<0.05$).

Effective Contribution of Human VPC-derived Vascular Cells for Vascular Regeneration

Fixed tissues harvested from ischemic hindlimbs at day 7 were inspected by the fluorescence stereomicroscope (Leica, Wetzlar,

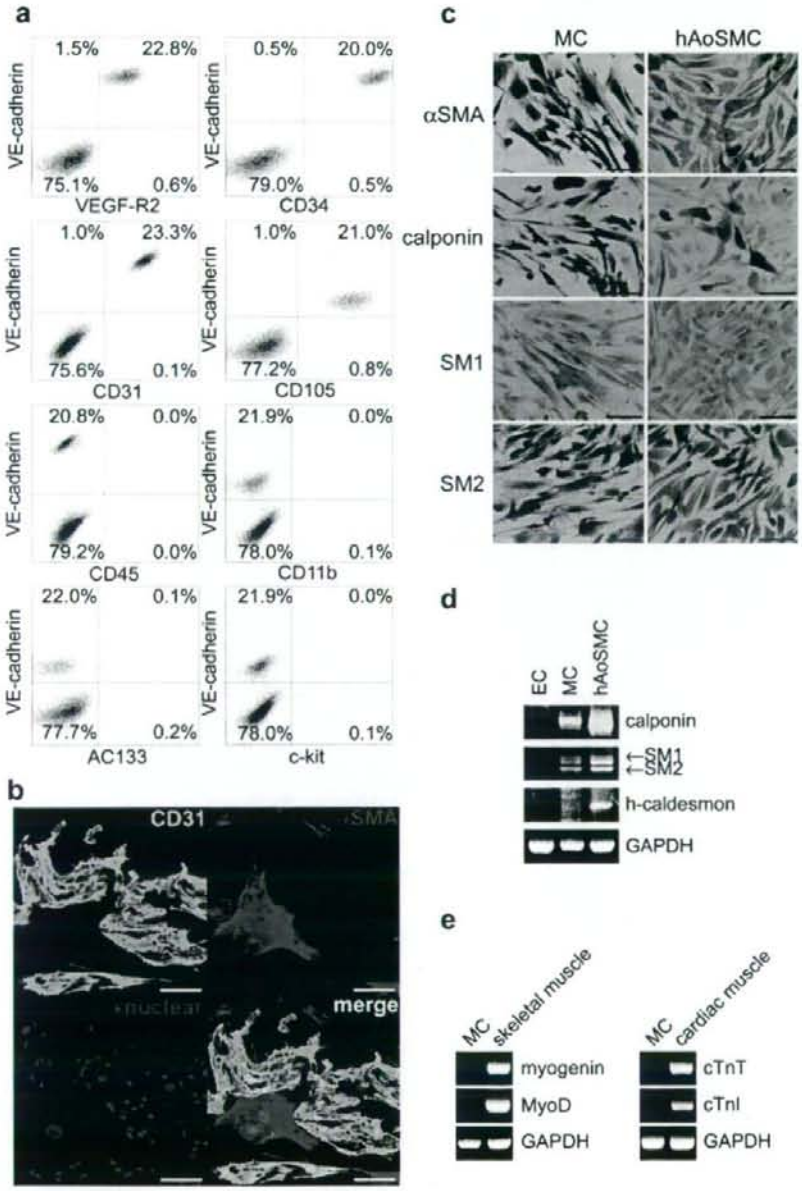

Figure 1. Characterization of transplanted human VPC-derived vascular cells. a) Flow cytometric analysis of cell surface markers on expanded human VPC-derived VEGF-R2$^+$VE-cadherin$^+$ cells (=EC). b) Immunofluorescence image of CD31 (green) and αSMA (red) with nuclear staining (blue) in expanded EC. Scale bar: 100 μm. c) Immunostaining of mural cell markers (brown) with hematoxyline counter-staining of expanded VPC-derived VEGF-R2$^+$VE$^-$cadherin- cells (=MC). Scale bar: 100 μm. d, e) RT-PCR analysis of mural cell (d) and skeletal/cardiac specific (e) markers in human VPC-derived vascular cells.

doi:10.1371/journal.pone.0001666.g001

Germany). Extended distribution of DiI-positive transplanted cells was clearly seen in both VPC-derived EC+MC and pEPC-transplanted hindlimbs (Figure 5a). We also detected some DiI-positive vessel-like formation in the lung and spleen, but no obvious tumor-like structures were seen (data not shown). Ischemic hindlimbs at day 14 were sectioned and treated with streptavidin conjugated dye to stain intravenously injected biotinylated isolectin B_4, followed by anti-human CD31 antibody, and scanned for the incorporation of transplanted cells into circulating vessels. In the EC+MC group, we found that human

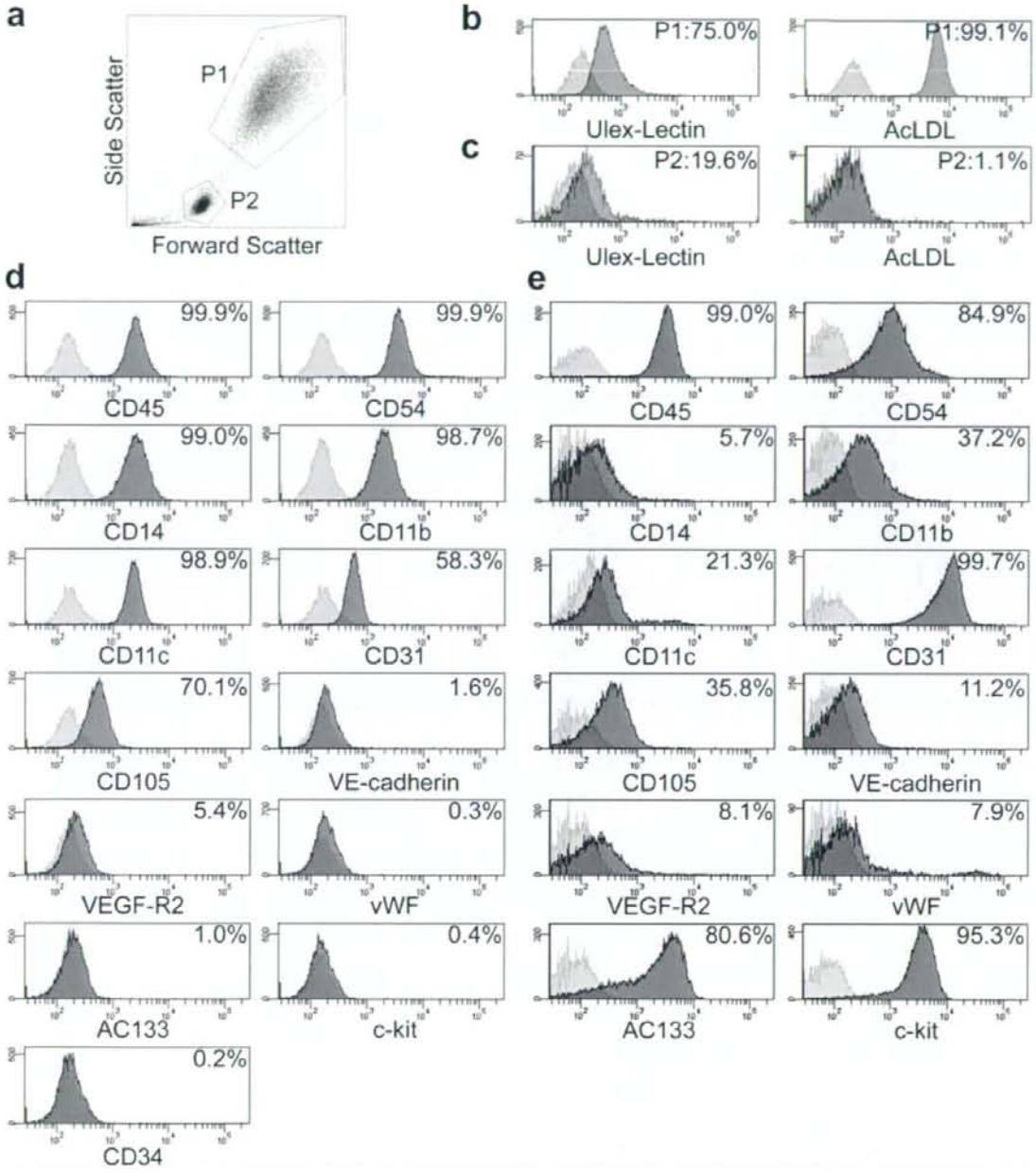

Figure 2. Characterization of peripheral blood and umbilical cord-derived EPC (pEPC and uEPC, respectively) by flow cytometer. a) Representative forward and side scatter profile of cultured pEPC. b-d) Flow cytometric analysis of ulex-lectin binding/acLDL uptake (b, c) and various cell surface markers (d) in pEPC. e) Flow cytometric analysis of cell surface markers in uEPC.
doi:10.1371/journal.pone.0001666.g002

CD31 positive cells formed capillaries with host EC, which were stained with isolectin B_4 (Figure 5b: arrowhead). Furthermore, some human CD31 positive cells solely formed capillary vessel (Figure 5b: arrow), which might indicate de novo vessel formation from human VPC-derived EC. We also detected human CD31 positive cells in the pEPC and uEPC group; however, many of these cells were located within the lumen of host capillaries (Figure 5c, arrow).

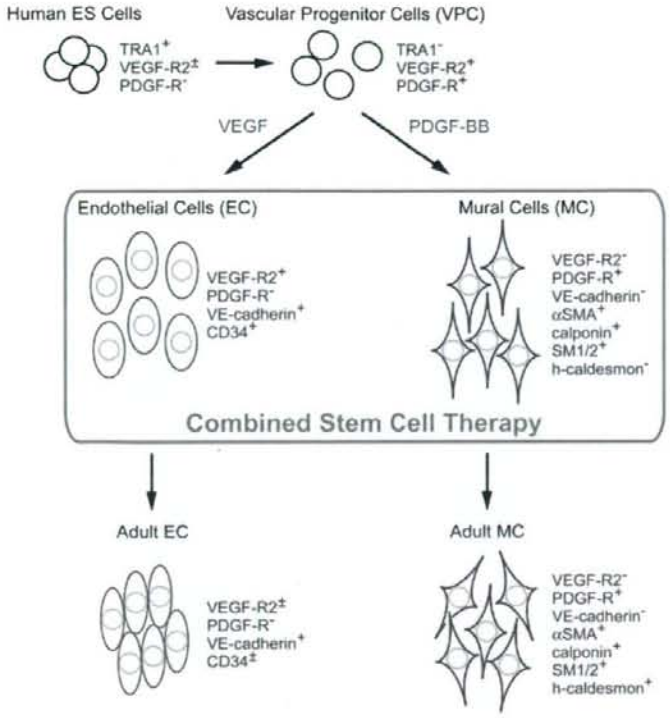

Figure 3. Possible differentiation pathway of vascular cells from human ES cells via VPC.
doi:10.1371/journal.pone.0001666.g003

We further investigated the contribution of transplanted VPC-derived MC to the recruitment of mural cells. We stained the sections of ischemic hindlimbs at day 14 with anti-human SM1 and αSMA antibodies. In EC+MC-transplanted mice, we found some human SM1 and αSMA double positive cells, which were localized within the αSMA positive host vessel wall (Figure 5d: arrow).

Quantification of Transplanted VPC-derived Vascular Cell-induced Vascular Regeneration in Ischemic Hindlimb

The sections of ischemic hindlimbs of the EC+MC group at day 42 were stained with anti-human and mouse CD31 antibodies. Mouse CD31 positive capillary density was significantly high in the EC+MC group ($1775.3\pm54.2/mm^2$), compared to other groups ($P<0.0001$ vs. control group: $1318.6\pm73.0/mm^2$) (Figure 6b). Human CD31 positive capillary density in mice transplanted with human VPC-derived EC (EC ($149.9\pm12.3/mm^2$) and EC+MC ($135.7\pm13.7/mm^2$) was significantly higher than that in mice transplanted with EPC ($95.7\pm8.5/mm^2$ in the pEPC and $115.2\pm12.0/mm^2$ in the uEPC group) ($P<0.05$). Compatible with the result of blood flow measurement, mouse and/or human CD31 positive capillary density markedly increased in mice that received human VPC-derived EC+MC ($1856.8\pm57.0/mm^2$) ($P<0.0001$, compared to the control group ($1318.6\pm73.0//mm^2$)), and also to other groups. Among the single cell transplantation groups, mouse and/or human CD31 positive capillary density increased in the EC group ($1601.4\pm51.4/mm^2$) ($P=0.0016$) compared to the control group, but did not increase in the MC ($1471.8\pm42.4/mm^2$) or EPC groups ($1403.5\pm84.4/mm^2$ in the pEPC and $1524.8\pm108.2/mm^2$ in the uEPC group).

To confirm the maturity of newly formed vessels, we performed the immunostaining of the ischemic tissues with anti-αSMA antibody, which could stain both human and mouse MC (Figure 6c). We confirmed that αSMA positive capillary density was significantly increased in the human VPC-derived vascular cells-transplanted groups (MC ($1317.6\pm45.4/mm^2$), EC ($1357.7\pm27.3/mm^2$) and EC+MC ($1554.9\pm48.8/mm^2$)) ($P<0.0001$), compared to the control group ($1021.3\pm46.3/mm^2$) (Figure 6d). Among the EPC groups, αSMA positive capillary density was significantly increased in the uEPC group ($1185.7\pm42.2/mm^2$) ($P<0.0076$) compared to the pEPC ($1118.9\pm36.8/mm^2$) and control group. We further investigated the extent of arteriogenesis in these groups using αSMA immunostaining sections. Many αSMA positive arterioles with more than 20 μm in diameter were detected in the EC+MC group, but not in the control group (Figure 6c: arrowhead). The number of αSMA positive arterioles significantly increased in the human VPC-derived vascular cells-transplanted groups, especially in the EC+MC group (the MC group:$4.0\pm0.3/mm^2$ and the EC group:$3.7\pm0.2/mm^2$; $P<0.001$, compared to the control group: $2.0\pm0.2/mm^2$, the EC+MC group: $5.5\pm0.7/mm^2$; $P<0.0001$, compared to all other groups) (Figure 6e). However, no significant difference in the number of αSMA positive arterioles was seen between the EPC (the pEPC group:$1.9\pm0.2/mm^2$ and the uEPC group:$2.0\pm0.2/mm^2$) and control groups.

Discussion

The present study demonstrated that the transplantation of human VPC-derived vascular cells at the proper differentiation

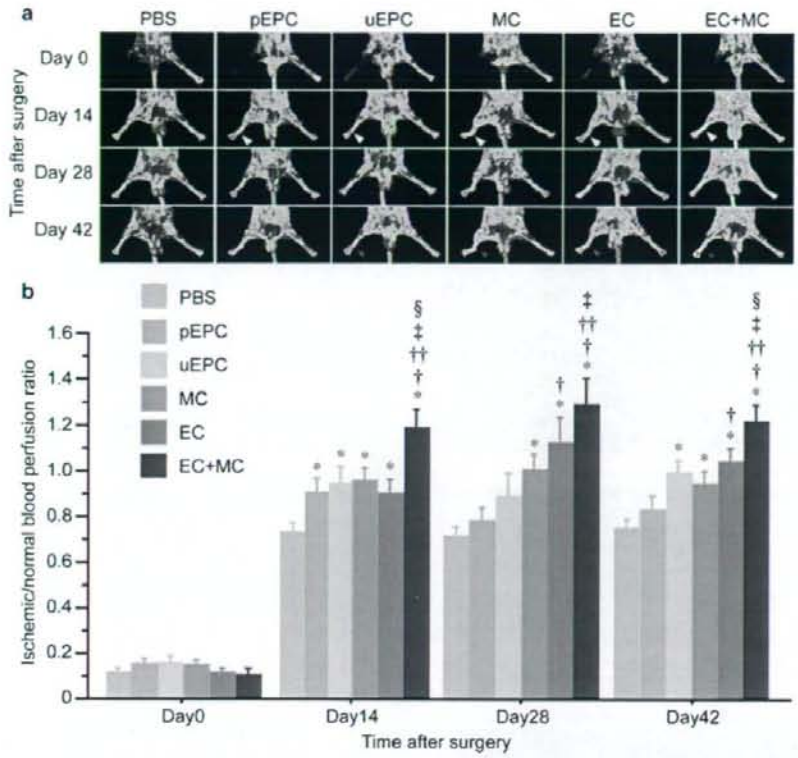

Figure 4. Augmented vascular regeneration by intra-arterial transplantation of human VPC-derived vascular cells in a murine hindlimb ischemia model. a) Serial LDPI analysis in hindlimb ischemia mice. At day 14, the blood flow of ischemic limbs in all cell transplanted groups increased significantly compared to the control group (white arrowhead). After 42 days, significant blood flow recovery was observed in the uEPC and human VPC-derived EC and/or MC-transplanted groups (red arrowhead), but not in pEPC. b) Quantitative analysis of hindlimb blood flow by calculating the ischemic/normal limb perfusion ratios after the induction of hindlimb ischemia. *$P<0.05$ vs. control, †$P<0.05$ vs. pEPC, ††$P<0.05$ vs. uEPC, ‡$P<0.05$ vs. MC, §$P<0.05$ vs. EC.
doi:10.1371/journal.pone.0001666.g004

stage successfully promoted vascular regeneration in the setting of tissue ischemia. After the expansion of human VPC-derived EC and MC, when intra-arterially administered, these cells significantly augmented neovascularization in an animal model of experimentally-induced hindlimb ischemia, compared to human peripheral blood and umbilical cord-derived EPC (pEPC and uEPC). Furthermore, the combined transplantation of human VPC-derived EC and MC could markedly induce vascular regeneration, compared to the single fraction transplantation of VPC-derived vascular cells (EC or MC). We also succeeded in demonstrating that transplanted human VPC-derived vascular cells were incorporated into the host circulation as both EC and MC. These results indicate that the combined transplantation of human VPC-derived EC and MC may have utility as a novel strategy for vascular regenerative medicine.

In the present study we used human VPC-derived VEGFR2$^+$ VE-cadherin$^+$ cells for the expansion and transplantation of EC. VEGFR2$^+$VE-cadherin$^+$ cells, obtained at day 10 of differentiation, were also positive for CD34 and therefore considered to be EC at the early differentiation stage (Figure 3) [9]. Even after 6 passages, 20~40% of these cells exhibited the expression of VEGFR2, VE-cadherin, and CD34, which indicated that they still retained the phenotype of EC at the early differentiated stage. Compared to EPC, transplantation of these EC significantly augmented ischemia-induced neovascularization. In contrast, we found that ischemia-induced neovascularization was not improved in mice receiving human aortic endothelial cells [4]. Therefore, human VPC-derived EC at the early differentiation stage might possess vascular regenerative capacity and these EC can be a valuable source for promoting vascular regeneration.

After expansion of human VPC-derived VEGFR2$^+$VE-cadherin$^+$ cells, about 70% of the expanded cells were αSMA positive. However, these cells were negative for the mature mural cell markers, including calponin, SM1, SM2, and h-caldesmon (data not shown). In contrast, expanded VEGFR2$^+$ VE-cadherin$^-$ cells obtained from human VPC under platelet derived growth factor (PDGF)-BB stimulation were positive for αSMA, calponin, SM1, and SM2, but negative for h-caldesmon. HAoSMC was positive for all of the mature MC markers, including h-caldesmon. In another series of our experiments, the mice receiving hAoSMC transplantation exhibited no significant improvement of neovascularization after the induction of ischemic hindlimbs (data not shown). Because h-caldesmon and calponin were reported to be expressed relatively late in SMC differentiation [10], human VPC-derived MC might be at a rather early "immature" differentiation

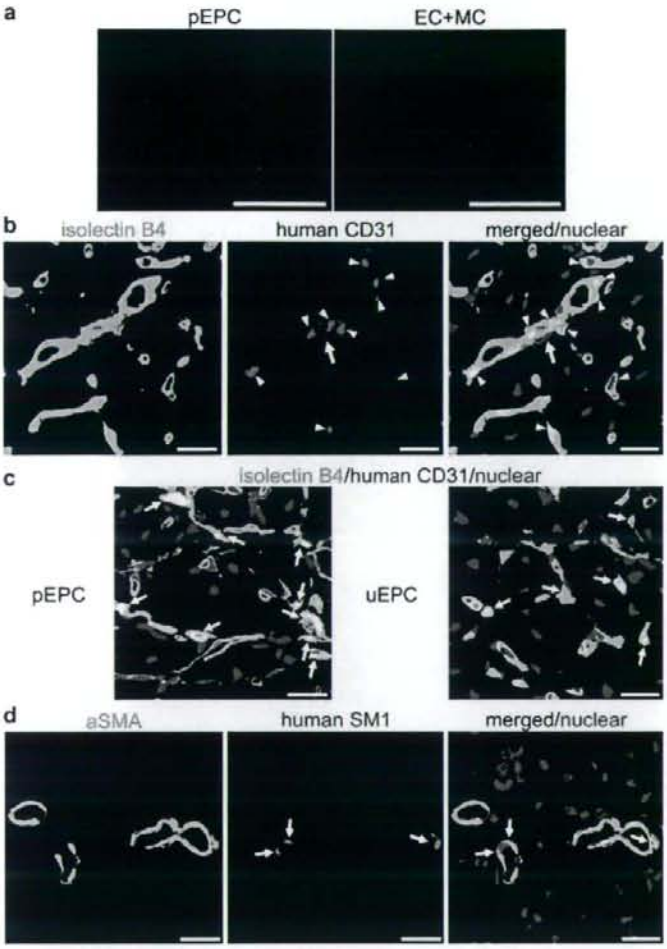

Figure 5. Incorporated human VPC-derived vascular cells at the sites of vascular regeneration. a) Transplanted CM-DiI (red) labeled pEPC or VPC-derived vascular cells in ischemic hindlimbs at day 7 were detected by the fluorescence stereomicroscope. Scale bar: 500 μm. b, c) Immunostaining of frozen sections harvested from ischemic limb tissues at day 14. Fluorescence staining of GSL I-isolectin B4 (green) and human CD31 (blue) with nuclear staining (red) in human VPC-derived EC+MC (b), pEPC, and uEPC (c) transplanted mice. Scale bar: 20 μm. d) Immunostaining of αSMA (green)/human SM1 (blue) with nuclear staining (red) in human VPC-derived EC+MC-transplanted mice at day 14. Scale bar: 20 μm.
doi:10.1371/journal.pone.0001666.g005

stage compared to hAoSMC, and thus, MC could be incorporated into the site of neovascularization.

Recently, Ferreira et al. reported that transplantation of human ES cells-derived EC into nude mice using Matrigel as scaffold contributed for the formation of blood vessels [11]. However, they did not show the direct integration of transplanted human ES cells-derived EC into host blood vessels. Judging from the double staining using intravenously injected isolectin B_4 and anti-human specific CD31 antibody, we found that the transplanted human VPC-derived EC incorporated into host circulating vessels. These transplanted EC could solely form de novo capillaries. In addition, by the double immunostaining of human SM1 and αSMA, we confirmed that transplanted human VPC-derived MC was also incorporated into host vessel walls. Therefore, transplanted human VPC-derived EC and MC structurally contributed to form new vessels in the process of vascular regeneration.

Interaction between EC and MC is essential for vascular development and maintenance of vascular stability [12,13]. Compared to only EC or MC-transplanted mice, the mice transplanted with the combined transplantation of EC and MC showed significant improvement after the induction of ischemic hindlimb. At day 42, the blood flow in the EC+MC group was significantly higher compared to only the EC or MC-transplanted groups. Not only mouse and/or human CD31 but also αSMA positive capillary density at day 42 significantly increased in the EC+MC group. We also found that the density of αSMA positive arterioles also significantly increased in the EC+MC group. These results indicated that combined transplantation of human VPC-derived EC and MC could synergistically contribute to vascular

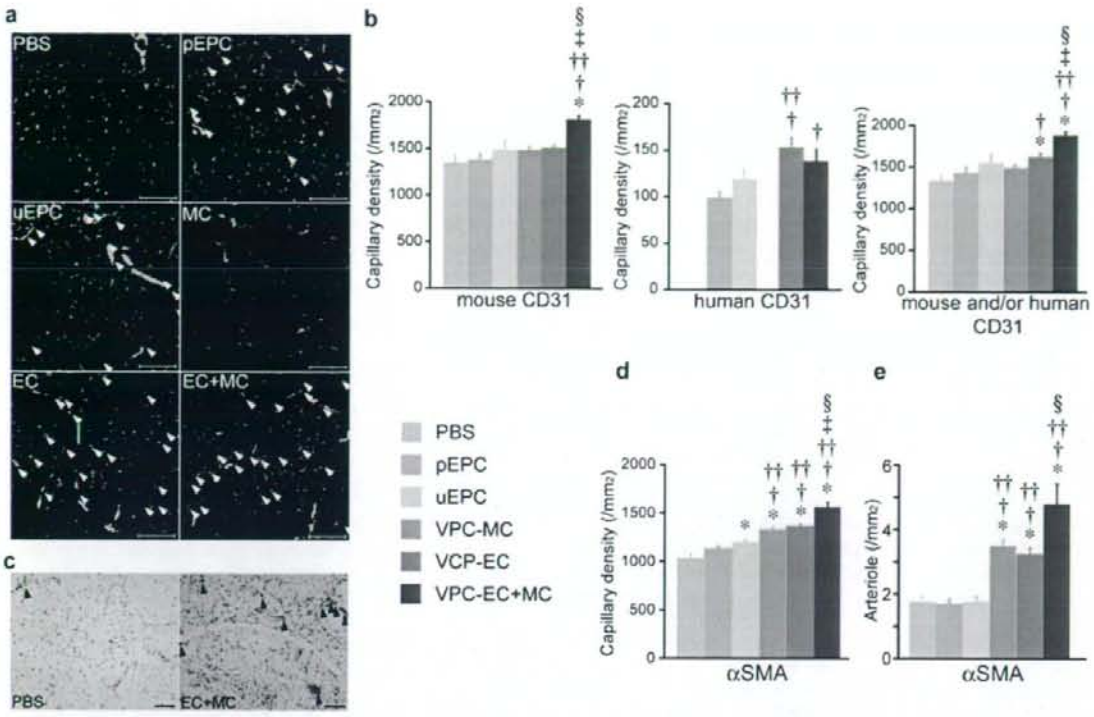

Figure 6. Immunohistochemical analysis of human VPC-derived vascular cells-transplanted murine hindlimb tissues. a) Representative fluorescent photographs of ischemic hindlimb stained for human (red) and mouse (green) CD31 at day 42. Overlapped-stained capillaries are shown in arrowhead. Scale bar: 100 μm. b) Quantitative analysis of the endothelial cell marker positive capillary density in ischemic hindlimbs at day 42. c) Representative αSMA immunostaining (brown) of ischemic hindlimbs at day 42. Scale bar. 100 μm. d) Quantitative analysis of αSMA positive capillary density in ischemic hindlimbs at day 42. e) Quantitative analysis of αSMA positive arterioles (black arrowhead) at day 42. *$P<0.05$ vs. control, †$P<0.05$ vs. pEPC, ††$P<0.05$ vs. uEPC, ‡$P<0.05$ vs. MC, §$P<0.05$ vs. EC.
doi:10.1371/journal.pone.0001666.g006

regeneration, and these MC could make mature blood vessels with adequate MC coating.

VEGFR2 is one of the most specific markers involved in the earliest stage of vascular endothelial and hematopoietic differentiation [14]. Recent reports suggest that VEGFR2$^+$ mesodermal progenitor cells also contribute muscle lineages including vascular smooth, skeletal, and cardiac muscles [1,15]. This evidence indicates the possibility that human VPC-derived MC, which were expanded from VEGFR2$^+$TRA1$^-$VE-cadherin$^-$ cells, might contain skeletal or cardiac muscle cells. However, 40-cycle RT-PCR was confirmed negative for skeletal and cardiac specific markers in expanded human VPC-derived MC. We cultured VPC-derived MC on dishes coated with collagen type IV, which is the major component of basement membrane. Previous reports described that basement membrane played an essential role in endothelial and smooth muscle cell differentiation [16]. Recently, Xiao et al. demonstrated that pretreatment of mouse ES cells with antibodies against collagen IV significantly inhibited smooth muscle cell differentiation [17]. They also demonstrated PDGF receptor-β signaling pathway plays a crucial role in ES cell-derived smooth muscle cell differentiation using PDGF receptor-β siRNA knockdown studies. Therefore, we suspected that, under the presence of collagen type IV and PDGF-BB, our human VPC-derived VE-cadherin negative cells could only differentiate to MC.

Human VPC-derived EC+MC-transplanted KSN nude mice showed considerable blood flow recovery, which led to more than 1.2 in the perfusion ratio of ischemic/non-ischemic limb. When we transplanted human VPC-derived vascular cells to immunosuppressed C57BL/6 mice, the perfusion ratio elevated to nearly 1 (data not shown). Therefore, the tendency of the blood flow recovery in C57BL/6 mice was consistent with the data of KSN nude mice, the absolute value of blood flow ratio after hindlimb ligation was different. Because both KSN nude and C57BL/6 mice received the same procedure for hindlimb ischemia, the degree of perfusion recovery after induction of hindlimb ischemia between these mice might reflect their difference in genetic background for angiogenesis, as reported by Fukino et al [18]. They demonstrated that the VEGF and VEGFR1/2 expression in response to ischemia was impaired in BALB/c mice, compared to other mouse strains (i.e, C57BL/6J or C3H/He mice). These results indicate that, because of the difference in genetic background, spontaneous collateral formation might be accelerated in our KSN nude mice compared to other strain mice.

In transplantation experiments, the number of mouse and/or human CD31 and mouse CD31-positive capillary density in the EC group was $1601.4\pm51.4/mm^2$ and $1470.1\pm41.6/mm2$, respectively. This difference in capillary density (1601.4–1470.1 = 131.3) was consistent with the number of human CD31-positive capillary density ($149.9\pm12.3/mm^2$). However,

compared to the EC group, the EC+MC group showed significant augmentation in mouse and/or human CD31 positive capillary density without the increase of human CD31 positive capillary density. One possible reason for this discrepancy is paracrine effects of transplanted human VPC-derived vascular cells might accelerate angiogenesis in ischemic tissues. We demonstrated that cultured human VPC-derived vascular cells expressed several angiogenic factors including VEGF, bFGF, HGF and PDGF-BB, and the release of VEGF from human VPC-derived vascular cells was significantly upregulated after transplantation (data not shown) [4]. Therefore, in addition to the structural contribution of transplanted human VPC-derived vascular cells into the host vascular network, the paracrine effects of these cells might enhance vascular regeneration in tissue ischemia.

Several reports described the contribution of pEPC or uEPC to neovascularization in tissue ischemia [6,7]. However, it has not been clearly demonstrated whether transplanted EPC augment neovascularization through differentiation and proliferation into mature EC or indirectly through paracrine stimulation of resident EC proliferation. Rehamn et al. demonstrated that the majority of pEPC, which were positive for acLDL and ulex-lectin, expressed monocyte/macrophage markers, and only a minority cell fraction expressed the specific endothelial or stem/progenitor markers [8]. They also demonstrated that pEPC did not proliferate, but released several potent angiogenic growth factors. In this study, we confirmed that a low percentage of cultured pEPC and uEPC expressed endothelial makers. A considerable number of pEPC or uEPC were localized inside the capillary lumen, not in the vessel wall. In addition, we found that VEGF mRNA expression in transplanted EPC was significantly higher compared with before transplantation (data not shown). These results suggest that the majority of EPC might have little ability to proliferate or differentiate to endothelial linage, and their angiogenic effects could be attributed to angiogenic factors secreted from transplanted EPC.

In conclusion, we have shown that human VPC-derived cells could effectively differentiate and be expanded to EC and MC. Combined transplantation of these "immature" VPC-derived vascular cells, unlike "mature" somatic EC and MC, augmented reparative neovascularization and contributed to make newly formed vessels in the murine hindlimb ischemia model far more effectively compared to EPC transplantation. Thus, human ES cells-derived EC and MC can be used as the new promising cell source for therapeutic vascular regeneration in patients with tissue ischemia in order to realize a novel combined stem cell therapy.

Materials and Methods

Differentiation of Human VPC-derived EC and MC

Maintenance of human ES cell line (HES3) was as previously described [19]. To induce VPC, undifferentiated ES cells were cultured on an OP9 feeder cell line as reported [3,4]. To obtain human VPC-derived EC, VEGFR2$^+$TRA1$^-$VE-cadherin$^+$ cells were sorted by fluorescence activated cell sorter (FACSAria; Becton Dickinson, Bedford, MA) at day 10 of differentiation, and cultured on type IV collagen-coated dishes (Becton Dickinson) in the presence of 10% FCS and 50ng/ml VEGF (human VEGF165, Peprotech Inc, Rocky Hill, NJ). After 6 passages of these cells, we re-sorted VE-cadherin$^+$ cells for transplantation of human VPC-derived EC. To expand human VPC-derived MC, sorted VEGFR2$^+$TRA1$^-$VE-cadherin$^-$ cells derived from VPC at day 8 were re-cultured on type IV collagen-coated dishes with 1% FCS and 20ng/ml human PDGF-BB (Peprotech Inc). We transplanted these human VPC-derived MC after 6 passages.

Preparation of Human EPC

Peripheral MNC-derived EPC (pEPC) were obtained from healthy volunteer, as previously described [6]. To confirm EPC phenotype, cells were detached with cell dissociation buffer (Invitrogen, Carlsbad, CA) and incubated with DiI-labeled acLDL (Invitrogen) and FITC-labeled Ulex europaeus agglutinin I (ulex-lectin) (Sigma-Aldrich, St. Louis, MO) for 1 hour. These cells were analyzed by FACSAria to be confirmed as EPC [6,8].

Umbilical cord blood-derived CD34$^+$ EPC (uEPC) were isolated from human umbilical cord blood, which were obtained from Cell Bank, RIKEN BioResource Center (Tukuba, Japan). CD34$^+$ cells were separated by a magnetic bead separation method using autoMACS system with direct CD34$^+$ progenitor cell isolation kit (Miltenyi Biotec GmbH, Gladbach, Germany) [7]. Protocols for using human umbilical cord blood were approved by the Ethics Committee of Kyoto University Graduate School of Medicine.

Characterization of VPC-derived Vascular Cells and EPC

To evaluate the surface marker phenotype of VPC-derived vascular cells and EPC, these cells were detached by cell dissociation buffer with or without collagenase (Wako Pure Chemical Industries, Osaka, Japan) and labeled for 15 minutes at 4°C with various fluorescence-conjugated monoclonal antibodies (Table 1) [20]. Cells were washed and analyzed on FACSAria flow cytometer with ≥30,000 events stored.

For the staining of cultured VPC-derived vascular cells on dishes, cells were stained with anti-human CD31 (WM59) (Becton Dickinson) antibody and several smooth muscle specific markers, as shown in Table 2. Cultured hAoSMC (Cambrex, East Rutherford, NJ) were used to obtain positive control staining.

For RT-PCR analysis, total RNA was prepared with RNeasy Mini Kit (QIAGEN Inc., Valencia, CA), and RT-PCR was performed by TaKaRa One Step RNA PCR Kit (TaKaRa Bio Inc., Otsu, Japan). Total RNA from human heart and skeletal muscle were purchased from Clontech (Mountain View, CA). Primers are listed in Table 3 [21–23].

Hindlimb Ischemia Model and Cell Transplantation

After 8-week-old male KSN/Slc nude mice (Japan SLC, Shizuoka, Japan) were anesthetized with pentobarbital (80mg/kg, i.p.), the right femoral vein was ligated. To transplant vascular cells intra-arterially, we injected these cells in 100 μl PBS into the right femoral artery. Immediately after the cell injection, the right femoral artery and vein were ligated and excised [24]. Animal procedures were performed according to Kyoto University standards for animal care.

Assessment of Transplanted Animals

The measurement of hindlimb blood flow was performed with a LDPI analyzer (Moor Instruments, Devon, United Kingdom), as previously described [24].

At arbitrary time points, biotin conjugated Griffonia simplicifolia lectin (GSL) I-isolectin B_4 (Vector Laboratories, Burlingame, CA) in 100 μl PBS was injected into the portal vein 15 minutes before sacrifice. Cryostat sections (10 μm thick) of the ischemic lower legs were stained with anti-mouse/human CD31 (clone WM59/Mec13.3) (Becton Dickinson) or anti-αSMA/human SM1 (clone 1A4/3F8) (DakoCytomation, Glostrup, Denmark/Yamasa Co., Tokyo, Japan) antibodies. For biotinylated isolectin B_4 staining to detect circulating vessels, sections were incubated with streptoavidin conjugated Alexa Fluor dye (Invitrogen).

Capillary densities were examined by counting the number of capillaries stained with anti-human and/or mouse CD31 or anti-

Table 1. Fluorescence-conjugated monoclonal antibodies used for FACS analysis

Antibody	Specificity	Clone	Conjugated fluorescence	Supplier
VEGF-R2	Endothelial cells	KM1998	Alexa Fluor 647	A generous gift of Prof. M. Shibuya, Tokyo University (Ref.20)
VE-cadherin	Endothelial cells	55-7H1	FITC or PE	Becton Dickinson, Bedford, MA
von Willebrand Factor (vWF)	Endothelial cells	2F2-A9	Alexa Fluor 488	Becton Dickinson, Bedford, MA
CD31 (PECAM1)	Endothelial cells or Monocytes	WM59	Alexa Fluor 488	eBioscience, San Diego, CA
CD105 (Endoglin)	Endothelial cells or Monocytes	266	Alexa Fluor 647	Becton Dickinson, Bedford, MA
CD11b (Mac1)	Monocytes	ICRF44	PE	eBioscience, San Diego, CA
CD11c	Monocytes	B-ly6	FITC	Becton Dickinson, Bedford, MA
CD14	Monocytes	M5E2	APC	Becton Dickinson, Bedford, MA
CD45	Panleukocytes	HI30	PE	Becton Dickinson, Bedford, MA
CD54 (ICAM-1)	Panleukocytes	581	PE	Becton Dickinson, Bedford, MA
AC133	Stem/Progenitor cells	AC133	PE	Miltenyi Biotec GmbH, Bergisch Gladbach, Germany
c-kit	Stem/Progenitor cells	YB5.B8	APC	Becton Dickinson, Bedford, MA
CD34	Stem/Progenitor cells	581	FITC	Becton Dickinson, Bedford, MA

doi:10.1371/journal.pone.0001666.t001

Table 2. Smooth muscle specific antibodies used for analysis

Antibody	Specificity	Clone	Supplier
Alpha smooth muscle actin (αSMA)	Human & mouse	1A4	DakoCytomation Denmark A/S, Glostrup, Denmark Sigma-Aldrich, St. Louis, MO
Calponin	Human	CALP	DakoCytomation Denmark A/S, Glostrup, Denmark
Smooth muscle myosin heavy chain 1 (SM1)	Human	3FB	Yamasa Co., Tokyo, Japan
Smooth muscle myosin heavy chain 2 (SM2)	Human & mouse	1G12	Yamasa Co., Tokyo, Japan

doi:10.1371/journal.pone.0001666.t002

Table 3. Primers for reverse transcription-polymerase chain reaction

Gene		Sequence	Length (bp)
Calponin[1]	Sense	5'-CTTCATGGACGGCCTCAAAGA-3'	713
	Antisense	5'-GTAGTTGTGTGCGTGGTGGTT-3'	
Smooth muscle myosin heavy chain 1 (SM1) and 2 (SM2)[1, 2]	Sense	5'-ATGAGGCCACGGAGAGCAACGA-3'	178 (SM1)
	Antisense	5'-CCATTGAAGTCTGCGTCTCGA-3'	217 (SM2)
h-caldesmon[1]	Sense	5'-AGACAAGGAAAGAGCTGAGGCA-3'	395
	Antisense	5'-GCTGCTTGTTACGTTTCTGCTC-3'	
Glyceraldehyde-3-phosphate dehydrogenase (GAPDH)[1]	Sense	5'-ACCACAGTCCATGCCATCAC-3'	452
	Antisense	5'-TCCACCACCCTGTTGCTGTA-3'	
Myogenin[3]	Sense	5'-GTGGGCGTGTAAGGTGTGTA-3'	141
	Antisense	5'-TGGTTGGGGTTGAGCAGGGT-3'	
MyoD[3]	Sense	5'-CCAAATGTAGCAGGTGTAAC-3'	142
	Antisense	5'-AGAGATAAATACAGCCCCAG-3'	
Cardiac troponin T (cTnT)[4]	Sense	5'-GGCAGCGGAAGAGGATGCTGAA-3'	150
	Antisense	5'-GAGGCACCAAGTTGGGCATGAACGA-3'	
Cardiac troponin I (cTnI)[4]	Sense	5'-CCCTGCACCAGCCCCAATCAGA-3'	250
	Antisense	5'-CGAAGCCCAGCCCGGTCAACT-3'	

[1]Ref. 21.
[2]We used a single pair of PCR primers that cover the sequence specific to SM2, because these two isoforms are produced from a single gene by alternative splicing.
[3]Ref. 22.
[4]Ref. 23.
doi:10.1371/journal.pone.0001666.t003

αSMA antibodies. Twenty (for CD31) or ten (for αSMA) random fields on two different sections (approximately 3mm apart) from each mouse were photographed and analyzed by NIH image as previously described [24].

Statistical Analysis

Results are presented as means±S.E.M. The serial changes of the hindlimb blood flow were assessed by repeated measures ANOVA, followed by Bonferoni's multiple comparison test. Comparisons among groups were tested by one-way ANOVA followed by Bonferoni's multiple comparison test. A P value <0.05 was considered significant.

Acknowledgments

The human ES cells (HES3) were provided by ES Cell International Pre Ltd., Singapore.

Author Contributions

Conceived and designed the experiments: KY HI KN MS JY TY TC KH DT KM KP NO NS NT YF. Performed the experiments: KY MS KH. Analyzed the data: KY. Wrote the paper: KY HI.

References

1. Yamashita J, Itoh H, Hirashima M, Ogawa M, Nishikawa S, et al. (2000) Flk1-positive cells derived from embryonic stem cells serve as vascular progenitors. Nature 408: 92–96.
2. Yurugi-Kobayashi T, Itoh H, Yamashita J, Yamahara K, Hirai H, et al. (2003) Effective contribution of transplanted vascular progenitor cells derived from embryonic stem cells to adult neovascularization in proper differentiation stage. Blood 101: 2675–2678.
3. Sone M, Itoh H, Yamashita J, Yurugi-Kobayashi T, Suzuki Y, et al. (2003) Different differentiation kinetics of vascular progenitor cells in primate and mouse embryonic stem cells. Circulation 107: 2085–2088.
4. Sone M, Itoh H, Yamahara K, Yamashita JK, Yurugi-Kobayashi T, et al. (2007) Pathway for differentiation of human embryonic stem cells to vascular cell components and their potential for vascular regeneration. Arterioscler Thromb Vasc Biol 27: 2127–2134.
5. Asahara T, Murohara T, Sullivan A, Silver M, van der Zee R, et al. (1997) Isolation of putative progenitor endothelial cells for angiogenesis. Science 275: 964–967.
6. Kalka C, Masuda H, Takahashi T, Kalka-Moll WM, Silver M, et al. (2000) Transplantation of ex vivo expanded endothelial progenitor cells for therapeutic neovascularization. Proc Natl Acad Sci U S A 97: 3422–3427.
7. Murohara T, Ikeda H, Duan J, Shintani S, Sasaki K, et al. (2000) Transplanted cord blood-derived endothelial precursor cells augment postnatal neovascularization. J Clin Invest 105: 1527–1536.
8. Rehman J, Li J, Orschell CM, March KL (2003) Peripheral blood "endothelial progenitor cells" are derived from monocyte/macrophages and secrete angiogenic growth factors. Circulation 107: 1164–1169.
9. Fina L, Molgaard HV, Robertson D, Bradley NJ, Monaghan P, et al. (1990) Expression of the CD34 gene in vascular endothelial cells. Blood 75: 2417–2426.
10. Frid MG, Shekhonin BV, Koteliansky VE, Glukhova MA (1992) Phenotypic changes of human smooth muscle cells during development: late expression of heavy caldesmon and calponin. Dev Biol 153: 185–193.
11. Ferreira LS, Gerecht S, Shieh HF, Watson N, Rupnick MA, et al. (2007) Vascular progenitor cells isolated from human embryonic stem cells give rise to endothelial and smooth muscle like cells and form vascular networks in vivo. Circ Res 101: 286–294.
12. Chan-Ling T, Page MP, Gardiner T, Baxter L, Rosinova E, et al. (2004) Desmin enshrathment ratio as an indicator of vessel stability: evidence in normal development and in retinopathy of prematurity. Am J Pathol 165: 1301–1313.
13. Hughes S, Chan-Ling T (2004) Characterization of smooth muscle cell and pericyte differentiation in the rat retina in vivo. Invest Ophthalmol Vis Sci 45: 2795–2806.
14. Nishikawa SI, Nishikawa S, Hirashima M, Matsuyoshi N, Kodama H (1998) Progressive lineage analysis by cell sorting and culture identifies FLK1+VE-cadherin+ cells at a diverging point of endothelial and hemopoietic lineages. Development 125: 1747–1757.
15. Motoike T, Markham DW, Rossant J, Sato TN (2003) Evidence for novel fate of Flk1+ progenitor: contribution to muscle lineage. Genesis 35: 153–159.
16. Sakata N, Kawamura K, Takebayashi S (1990) Effects of collagen matrix on proliferation and differentiation of vascular smooth muscle cells in vitro. Exp Mol Pathol 52: 179–191.
17. Xiao Q, Zeng L, Zhang Z, Hu Y, Xu Q (2007) Stem cell-derived Sca-1+ progenitors differentiate into smooth muscle cells, which is mediated by collagen IV-integrin alpha1/beta1/alphav and PDGF receptor pathways. Am J Physiol Cell Physiol 292: C342–352.
18. Fukino K, Sata M, Seko Y, Hirata Y, Nagai R (2003) Genetic background influences therapeutic effectiveness of VEGF. Biochem Biophys Res Commun 310: 143–147.
19. Reubinoff BE, Pera MF, Fong CY, Trounson A, Bongso A (2000) Embryonic stem cell lines from human blastocysts: somatic differentiation in vitro. Nat Biotechnol 18: 399–404.
20. Sawano A, Iwai S, Sakurai Y, Ito M, Shitara K, et al. (2001) Flt-1, vascular endothelial growth factor receptor 1, is a novel cell surface marker for the lineage of monocyte-macrophages in humans. Blood 97: 785–791.
21. Miwa Y, Sasaguri T, Inoue H, Taba Y, Ishida A, et al. (2000) 15-Deoxy-Delta(12,14)-prostaglandin J(2) induces G(1) arrest and differentiation marker expression in vascular smooth muscle cells. Mol Pharmacol 58: 837–844.
22. Kato H, Ohta S, Koshida S, Narita T, Taga T, et al. (2003) Expression of pericyte, mesangium and muscle markers in malignant rhabdoid tumor cell lines: differentiation-induction using 5-azacytidine. Cancer Sci 94: 1059–1065.
23. Kehat I, Kenyagin-Karsenti D, Snir M, Segev H, Amit M, et al. (2001) Human embryonic stem cells can differentiate into myocytes with structural and functional properties of cardiomyocytes. J Clin Invest 108: 407–414.
24. Yamahara K, Itoh H, Chun TH, Ogawa Y, Yamashita J, et al. (2003) Significance and therapeutic potential of the natriuretic peptides/cGMP/cGMP-dependent protein kinase pathway in vascular regeneration. Proc Natl Acad Sci U S A 100: 3404–3409.

EXPERIMENTAL CELL RESEARCH 314 (2008) 939–949

available at www.sciencedirect.com

ScienceDirect

www.elsevier.com/locate/yexcr

Research Article

Identification of adherens junction-associated GTPase activating proteins by the fluorescence localization-based expression cloning

Miho Matsuda[a,1,2], *Yuka Kobayashi*[a,1,3], *Sayuri Masuda*[a,b], *Makoto Adachi*[a], *Tsuyoshi Watanabe*[b], *Jun K. Yamashita*[c], *Eiichiro Nishi*[d], *Shoichiro Tsukita*[a], *Mikio Furuse*[b,*]

[a]*Department of Cell Biology, Graduate School of Medicine, Kyoto University, Yoshida-Konoe, Sakyo-ku, Kyoto 606-8501, Japan*
[b]*Division of Cell Biology, Department of Physiology and Cell Biology, Kobe University Graduate School of Medicine, 7-5-1 Kusunoki-cho, Chuo-ku, Kobe 650-0017, Japan*
[c]*Laboratory of Stem Cell Differentiation, Stem Cell Research Center, Institute of Frontier Medical Sciences, Kyoto University, 53 Kawahara-cho, Shogoin, Sakyo-ku, Kyoto 606-8507, Japan*
[d]*Molecular Pathology Unit, Horizontal Medical Research Organization, Graduate School of Medicine, Kyoto University, Yoshida-Konoe, Sakyo-ku, Kyoto 606-8501, Japan*

ARTICLE INFORMATION

Article Chronology:
Received 24 March 2007
Revised version received
19 October 2007
Accepted 12 November 2007
Available online 19 November 2007

Keywords:
Junctional complex
Adherens junctions
Tight junctions
FL-REX
GFP
GAP
ARHGAP12
SPAL3
Rap1

ABSTRACT

The junctional complex, including tight junctions (TJs), adherens junctions (AJs), and desmosomes, plays crucial roles in the structure and functions of epithelial cellular sheets. In this study, we evaluated the fluorescence localization-based retrovirus-mediated expression cloning (FL-REX) method as an approach to identify novel molecular components of TJs and AJs. Using an expression library of cDNA–GFP-fusions derived from mRNA of a mouse epithelial cell line, we confirmed that cDNAs for various known TJ- and AJ-components could be cloned in the FL-REX. Furthermore, cDNAs for ARHGAP12 and SPAL3, two putative GTPase activating proteins (GAPs) for small G proteins, were cloned as novel components of the junctional complex. Immunofluorescence staining using antibodies generated in-house demonstrated that these GAPs were localized at epithelial cell–cell junctions in various mouse tissues, and were specific to AJs when observed under confocal laser-scanning microscopy. These data suggest that FL-REX is a powerful tool to identify novel proteins localized at TJs and AJs.

* *Corresponding author.* Fax: +81 78 382 5805.
E-mail address: furuse@med.kobe-u.ac.jp (M. Furuse).
[1] These two authors contribute equally in this work.
[2] Present address: Laboratory of Molecular Genetics, NICHD, National Institute of Health, Bethesda, MD 20892, USA.
[3] Yuka Kobayashi's present address is Research Unit for Immune Tissue Engineering, Research Center for Allergy and Immunology, RIKEN Yokohama Institute,1-7-22 Suehiro-cho, Tsurumi,Yokohama 230-0045, Japan.

0014-4827/$ – see front matter © 2007 Elsevier Inc. All rights reserved.
doi:10.1016/j.yexcr.2007.11.009